2.13 MULTIPATH AND DIFFRACTION

Multipath is an interference condition that usually occurs at low tracking altitudes when reflected energy is received from round-trip paths other than direct reflection. The most severe tracking errors result from the ground path reflection geometry shown in Figure 2.13-1.

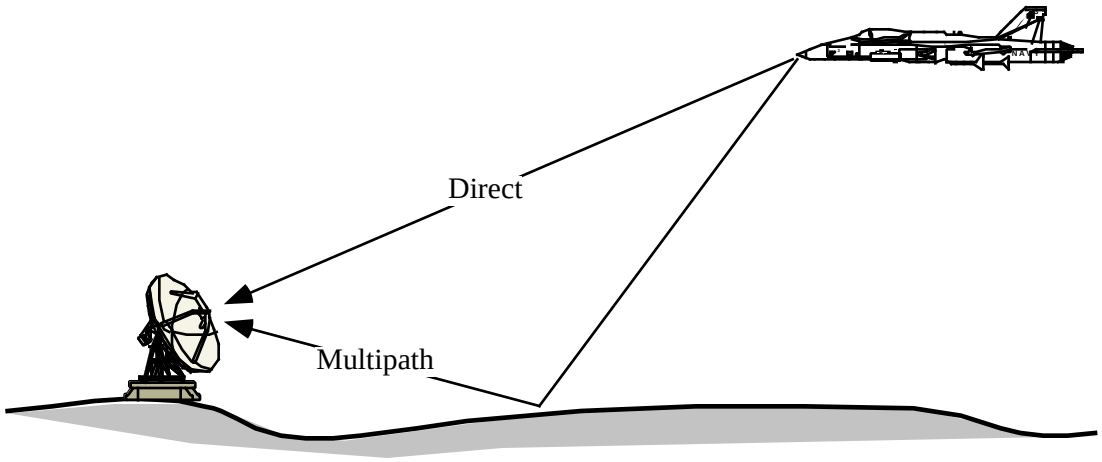

FIGURE 2.13-1. Ground Reflection Multipath.

For pulsed systems, ground reflection introduces a pulse return delay introducing range error and a reflection image at a lower elevation angle resulting in an elevation error.

Multipath effects generally arise from two types of scattering processes, specular and diffuse. Specular scattering is largely due to smooth surface reflection and can be accounted for as a coherent signal return from a geometric point source whereas diffuse scattering results from rough surfaces and is characterized by noncoherent reflection over a somewhat broad surface area (see Reference 9). Specular multipath effects range and elevation tracking while diffuse multipath contributes to azimuth as well as elevation and range errors.

The power and direction of return of multipath signals are determined by the radar range equation, path geometry and scattering surface properties. The radar range equation accounts for signal strength at the target and scattering points. Path geometry dictates range distances, phase shift due to path length differences and directional transmitter and receiver gain coefficients. Scattering surface properties include surface location and orientation and roughness factors. The amount of energy reflected from a surface element is characterized by a reflection coefficient which is a function of surface roughness, wave polarization and vegetation.

The intent of the multipath implementation is to generate realistic signal returns that would result from multipath propagation effects during low altitude tracking situations. ESAMS will compute signal return contributions from both specular and diffuse scattering sources accounting for target signature, position and velocity and physical characteristics and orientation of the scattering terrain.

Two independent models will implement multipath in ESAMS. The first is referred to as the Native multipath implementation and is based on algorithms developed at the Georgia

Institute of Technology and originally installed in the TAC ZINGER models. The second uses output data from the Ground Radar Clutter Estimator (GRACE). The GRACE option is based on the multipath methodology developed at Lincoln Laboratories as installed in the ACES/Phoenix modeling environment.

Diffraction effects are not modeled in ESAMS.

2.13.1 Functional Element Design Requirements

This section discusses the design requirements for the multipath functional element for both the native and the GRACE multipath implementations.

2.13.1.1 Native Multipath Design Requirements

a. The native multipath implementation will generate simulated signal returns from specular and diffuse scattering sources.

b. For the native multipath, the scattering terrain will be represented by a number of terrain facet elements. For a given site-target location, multipath signal return will be computed by examining all terrain facets along a line segment joining the radar site and the ground position of the target for specular and diffuse contributions.

c. The native multipath implementation will generate specular and diffuse multipath signal returns as a result of forward scattering over the following user selectable terrain types: sea, soil, grass, crops, sand, rocks, urban areas, and snow.

   Terrain facet data will contain data related to electromagnetic reflectivity. The multipath functional element will account for this reflective property by computing the appropriate reflection coefficient as a function of terrain type for each terrain facet supporting multipath contributions.

d. The native multipath implementation will generate specular and diffuse multipath signals as a result of forward scattering over terrain of user selectable roughness.

   Terrain facet data will contain RMS surface height variation and correlation distance data. The RMS slope of surface irregularities as a function of height variation and correlation distance will be used as a factor in the reflection coefficient.

e. The native multipath implementation will compute the centroid of the Doppler shift of the multipath signal return over the scattering terrain.

   Target location and speed along with facet location relative to the radar site will be used to compute a centroid of the Doppler frequency shift induced by target motion relative to the terrain. This Doppler shift will in turn be used to determine the appropriate MTI filter attenuation.

GRACE Multipath Design Requirements

a. The GRACE multipath implementation will generate simulated signal returns from specular and diffuse scattering sources.

b. For GRACE multipath, the scattering terrain will be represented by SITE MASK data given as a set of radials containing patches of terrain that can be illuminated from the radar site. The GRACE option will calculate the amount of specular and diffuse multipath signal return by computing the sum and difference channel voltage at each illumination patch along each radial.

c. The GRACE option for multipath implementation will compute the centroid of the Doppler shift of the multipath signal return over the scattering terrain.

d. Target location and speed along with facet location relative to the radar site will be used to compute a centroid of the Doppler frequency shift induced by target motion relative to the terrain. This Doppler shift will in turn be used to determine the appropriate MTI filter attenuation.

2.13.2 Functional Element Design Approach

Section 2.13.2 contains descriptions of the design elements used to satisfy the design requirements for both the native and GRACE multipath implementations. A design element is an algorithm or feature that represents a specific component of the FE design.

Native Multipath Design

For native multipath, the surface of the Earth in ESAMS is represented by a grid of square terrain facets measuring 500 meters on each side. Associated with each terrain facet is a set of data describing the orientation and physical characteristics of the facet element. Terrain facet data is arranged as a two dimensional array, IFACET(I,J), where J is the facet number, and I indexes facet data (Table 2.13-1).

TABLE 2.13-1. Terrain Facet Array Data.

I	F(I,J) Data Description
1	Transverse tilt of facet element J
2	Longitudinal tilt of facet element J
3	RMS slope of the facet surface irregularities
4	Terrain type code
5	Shadow flag1: facet is shadowed 0: facet not shadowed

Currently, the native code is not capable of processing digitized terrain and, therefore, must be used with the default flat-earth methodology. Thus, the transversal tilts and the shadow flag values are always zero. The code for determining shadowing (masking) is still included in ESAMS, but it is not described in this document because it always determines that no facets are shadowed. The values of the array for I=3 and I=4 are used to determine the reflectivity of each facet.

Specular and diffuse multipath contribution will be determined by connecting a line segment along the ground between the radar site and the ground position of the target as shown in Figure 2.13-2. Only facets intersected by this line segment will be considered as candidates for multipath contribution. The minimum required conditions for a particular facet to support multipath are that a minimum amount of site-to-target ground line intersects the facet, and the facet is less than twenty beamwidths (half-power angles) off of the antenna boresight. If these conditions are not met, then neither specular nor diffuse

multipath will be computed for the facet element. If the minimum conditions are met, then a diffuse component is assumed to be present and a specular contribution may be present.

If it is determined that a particular facet will support multipath, then the length of the line segment that intersects the facet will be retained for use as a weighing factor for the specular and diffuse reflection coefficients.

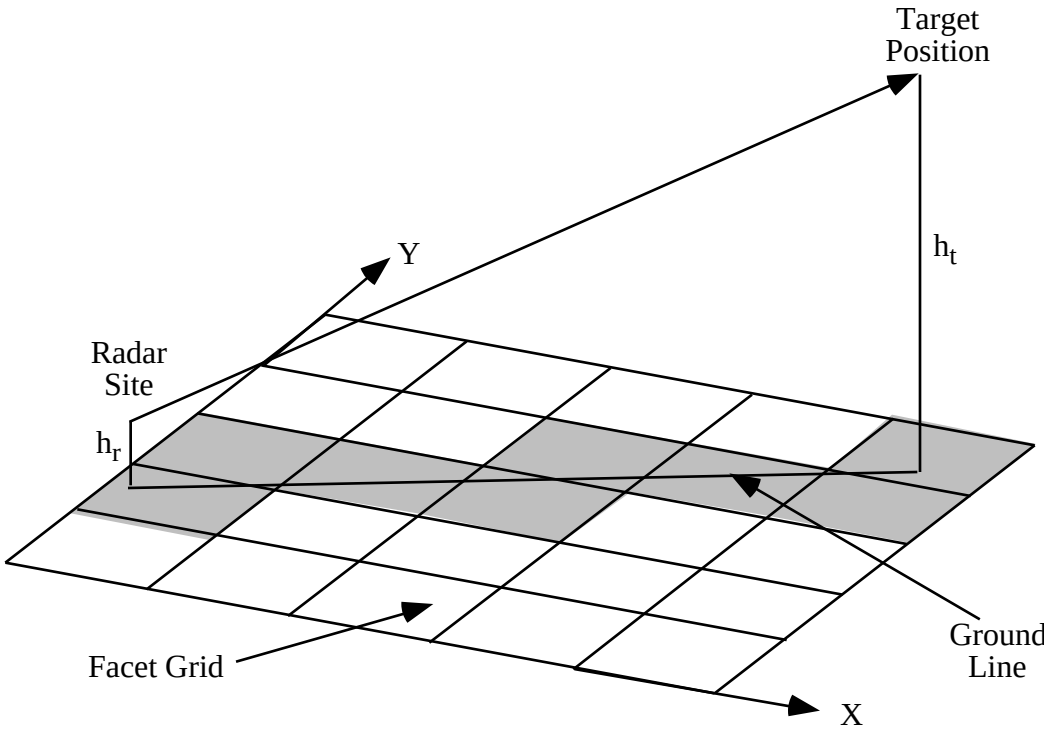

FIGURE 2.13-2. Radar Site, Terrain Facet Grid and Target Geometry.

In Figure 2.13-2, terrain facets suitable for multipath consideration appear shaded. These facets are determined by examining the site-to-target ground line segments as they intersect the borders of the facet grid. This process is described in the first four design elements below.

Design Element 13-1: Grid Geometry Initialization

Native multipath geometric calculations use grid coordinates rather than the model standard coordinates (measured in meters). The length of a facet side is used as the unit of measure. One of the first steps is to convert standard parameters into grid units by dividing by L, where L = length of a facet side (meters); L is set to 500 m in ESAMS as delivered. All linear variables in this mode are assumed to be measured in grid units unless otherwise specified. Standard descriptions of ground (horizontal) distances between the site and the target are given below.

$$\Delta x = x_t - x_r$$
$$\Delta y = y_t - y_r \qquad [2.13\text{-}1]$$
$$G = \sqrt{\Delta x^2 + \Delta y^2}$$

where (x_t,y_t) = target coordinates (grid units)
(x_r,y_r) = radar site coordinates (grid units)

For determining facets that contribute to multipath, the grid coordinates are bounded by Rmax, the range to the horizon from the site. The following equation is based on page 127 of Barton (Reference 10).

$$R_{max} = \frac{\sqrt{2KR_E h_r}}{L} \qquad [2.13\text{-}2]$$

where K = refractivity factor (4/3)
R_E = radius of the earth (m)
h_r = antenna height (m)
L = factor for conversion to grid units (m)

Therefore,

$$(x_{max}, y_{max}) = \begin{cases} (x_t, y_t), & \text{if } G \le R_{max} \\ \left(\frac{\Delta x R_{max}}{G}, \frac{\Delta y R_{max}}{G}\right), & \text{otherwise} \end{cases} \qquad [2.13\text{-}3]$$

The last step is to find the integer coordinates (x_{end},y_{end}) of the farthest corner of the facet containing (x_{max},y_{max}).

$$x_{end} = \begin{cases} \|x_{max}\|, & \text{if } x_{max} < 0 \\ \|x_{max}\| + 1, & \text{if } x_{max} \ge 0 \end{cases}$$

$$y_{end} = \begin{cases} \|y_{max}\|, & \text{if } y_{max} < 0 \\ \|y_{max}\| + 1, & \text{if } y_{max} \ge 0 \end{cases} \qquad [2.13\text{-}4]$$

where $\| \ \|$ indicates the greatest integer function.

Design Element 13-2: Intercept Arrays

Two arrays are defined to describe how the ground line from the site to the target intersects the facet grid lines: P_1(j,k) gives the first intercept of the ground line with the grid lines, starting from the radar site (x_s,y_s), and U(j,k) gives the unit coordinate array that describes the coordinate increment from one grid line intercept to the next.

The array P_1(j,k) is described as follows:

$P_1(1,1)$ = x-coordinate of the first vertical grid line intercept
$P_1(1,2)$ = y-coordinate of the first vertical grid line intercept
$P_1(2,1)$ = x-coordinate of the first horizontal grid line intercept
$P_1(2,2)$ = y-coordinate of the first horizontal grid line intercept

It is easy to see that

$$P_1(1,1) = \begin{cases} \lfloor x_r \rfloor, & \text{if } \Delta x < 0 \\ \lfloor x_r \rfloor + 1, & \text{if } \Delta x \geq 0 \end{cases}$$

and

$$P_1(2,2) = \begin{cases} \lfloor y_r \rfloor, & \text{if } \Delta y < 0 \\ \lfloor y_r \rfloor + 1, & \text{if } \Delta y \geq 0 \end{cases} \qquad [2.13\text{-}5]$$

Note that $P_1(1,1)$ and $P_1(2,2)$ are undefined if $\Delta x = 0$, because there are no vertical grid line crossings if the site and target have the same x-coordinates. Similarly, $P_1(2,1)$ and $P_1(2,2)$ are undefined if $\Delta y = 0$.

The y-coordinate of the vertical grid line intersection and the x-coordinate of the horizontal grid line intersection are computed using the equation of a line through a point:

$$P_1(1,2) = y_r + \frac{\Delta y}{\Delta x}\left(P_1(1,1) - x_r\right), \quad \Delta x \neq 0$$

$$P_1(2,1) = x_r + \frac{\Delta x}{\Delta y}\left(P_1(2,2) - y_r\right), \quad \Delta y \neq 0 \qquad [2.13\text{-}6]$$

The unit increment array U(i,j) is described as follows:

$U(1,1)$ = horizontal distance from one vertical grid line intercept to the next
$U(1,2)$ = vertical distance from one vertical grid line intercept to the next
$U(2,1)$ = horizontal distance from one horizontal grid line intercept to the next
$U(2,2)$ = vertical distance from one horizontal grid line intercept to the next

From simple geometric considerations, it is easy to see that

$$U(1,1) = sign(\Delta x), \text{ if } \Delta x \neq 0$$
$$U(1,2) = \frac{\Delta y}{|\Delta x|}, \text{ if } \Delta x \neq 0$$
$$U(2,1) = \frac{\Delta x}{|\Delta y|}, \text{ if } \Delta y \neq 0 \qquad [2.13\text{-}7]$$
$$U(2,2) = sign(\Delta y), \text{ if } \Delta y \neq 0$$

As before, U(1,k) is undefined if $\Delta x = 0$, and U(2,k) is undefined if $\Delta y = 0$.

Design Element 13-3: Next Facet Segment

After finding P_1(j,k) and U(j,k) above, ESAMS enters a loop to step from one facet to the next along the site-target ground line. The first pass through the loop is entered with the current position at the radar site ground position, so the next vertical and horizontal grid line intersection coordinates are given by P_1(j,k). In later passes through the loop, the next vertical and horizontal grid line coordinates will be given by P_i(j,k) as determined by

Design Element 13-4 below. In either case, the next facet is found by determining which grid line intersection, vertical or horizontal, is closer to the current point (x_1,y_1). That intersection becomes the next point examined, (x_2,y_2). It is found as follows:

$$(x_2, y_2) = \begin{cases} (P_i(1,1), P_i(1,2)), & \text{if } sign(\Delta x) P_i(1,1) \le sign(\Delta x) P_i(2,1) \\ (P_i(2,1), P_i(2,2)), & \text{otherwise} \end{cases} \quad [2.13\text{-}8]$$

The line segment from (x_1,y_1) to (x_2,y_2) crosses a facet. To ensure that this line segment should be considered for multipath, the farthest corner (x_c,y_c) of this facet is found and compared to the farthest corner (x_{end},y_{end}) containing the maximum range (see Equations [2.13-3] and [2.13-4]).

$$x_c = trunc\left[\frac{1}{2}(x_1 + x_2 + 1)\right]$$
$$y_c = trunc\left[\frac{1}{2}(y_1 + y_2 + 1)\right] \quad [2.13\text{-}9]$$

where *trunc* indicates the truncation function.

If (x_c,y_c) is beyond the facet containing the maximum range, then the next point is changed from the grid line intersection to the point on the ground line at the maximum range.

If $x_c \ge x_{end}$ and $y_c \ge y_{end}$
Then, $(x_2,y_2) = (x_{max},y_{max})$ [2.13-10]

The length of the ground line segment across this ith facet is then computed as usual.

$$g(i) = \sqrt{(x_2 - x_1)^2 + (y_2 - y_1)^2} \quad [2.13\text{-}11]$$

If this length is very small, then the facet is not considered for multipath contributions, and the next facet is considered as the ith facet.

If $g(i) < 0.01$, then do not enter data for this facet into the facet array [2.13-12]

Design Element 13-4: Next Intercept

The last procedure in the loop that steps from facet to facet along the ground line is to determine the values in the array P_{i+1}(j,k) that points to the next grid line intersections and to make the "next point" into the "current point" for the next pass through the loop.

If (x_2,y_2) is a vertical grid line intersection, then the next horizontal intersection is unchanged. Similarly, if (x_2,y_2) is a horizontal grid line intersection, then the next vertical intersection is unchanged. The one that is changed used the unit increment arrays from Design Element 13-2.

$$P_{i+1}(1,1) = \begin{cases} P_i(1,1), & \text{if } (x_2, y_2) = (P_i(2,1), P_i(2,2)) \\ x_2 + U(1,1), & \text{otherwise} \end{cases}$$

$$P_{i+1}(1,2) = \begin{cases} P_i(1,2), & \text{if } (x_2, y_2) = (P_i(2,1), P_i(2,2)) \\ y_2 + U(1,2), & \text{otherwise} \end{cases}$$

$$P_{i+1}(2,1) = \begin{cases} P_i(2,1), & \text{if } (x_2, y_2) = (P_i(1,1), P_i(1,2)) \\ x_2 + U(2,1), & \text{otherwise} \end{cases} \qquad [2.13\text{-}13]$$

$$P_{i+1}(2,2) = \begin{cases} P_i(2,2), & \text{if } (x_2, y_2) = (P_i(1,1), P_i(1,2)) \\ y_2 + U(2,2), & \text{otherwise} \end{cases}$$

Design Elements 13-1 through 13-4 are performed in a loop that finds all facets between the site and the target (or the horizon) that have a large enough intersection with the site-target ground line to produce multipath. All of these facets will be assumed to produce diffuse multipath returns. The next step is to determine which of them produce specular multipath returns.

Design Element 13-5: Specular Geometry

The first requirement for the presence of a specular component at a particular facet is that the return falls within the receiver range gate. This condition is considered to be met when the specular return arrives within one half of a pulse width of the direct return. The line-of-sight range, R, from the radar site to the target is given by:

$$R = \sqrt{G^2 + (h_r - h_t)^2} \qquad [2.13\text{-}14]$$

where: h_r = altitude of the radar site (grid units)

h_t = altitude of the target (grid units)

G = ground range from radar site to target (grid units)

The range to each facet is defined to be the range to the center of the ground line segment in the facet. Thus, the ground range from the radar site to the facet is defined recursively as follows:

$$G_r(1) = \frac{g(1)}{2}$$

$$G_r(i+1) = G_r(i) + \frac{1}{2}\left[g(i) + g(i+)\right] \qquad [2.13\text{-}15]$$

where $g(i)$ = length of ground line segment in ith facet (see Equation [2.13-11])

The ground range from the target to the facet is then obtained by subtraction.

$$G_t(i) = G - G_r(i) \qquad [2.13\text{-}16]$$

Next, the line-of-sight ranges to each facet are determined.

$$R_r(i) = \sqrt{G_r(i)^2 + \left(h_r - h(i)^2\right)}$$

$$R_t(i) = \sqrt{G_t(i)^2 + \left(h_t - h(i)^2\right)} \qquad [2.13\text{-}17]$$

where R_r = line-of-sight range from site to facet
R_t = line-of-sight range from target to facet
h_r = altitude of radar site
h_t = altitude of target
$h(i)$ = altitude of facet

Note again that all lengths are in grid units.

Now the path length difference, δ, between the direct and multipath returns can be computed by:

$$\delta_i = R_r(i) + R_t(i) - R \qquad [2.13\text{-}18]$$

If this path length difference is greater than the distance traveled by a propagating wave in a time span equal to one half of a pulse width, then the facet element is incapable of supporting specular multipath and is ignored in further multipath computations.

$$\text{If } \delta_i \geq c\tau/2, \text{ then there is no specular return from facet } i \qquad [2.13\text{-}19]$$

The second requirement for the presence of specular multipath is that the difference between the "grazing" angles from the radar site and from the target at the facet edges be small compared to the RMS slope of the surface irregularities, β_0, or that this difference vanish between the edge points. If the difference is small relative to β_0, then an amount of incident energy will be specularly reflected as a function of the RMS surface height variation, σ_h. The RMS slope of the surface irregularities is given by:

$$\beta_0 = \frac{2\sigma_h}{d_c} \qquad [2.13\text{-}20]$$

where: d_c = correlation

Geometry for line-of-sight rays from the radar and from the target to the facet is shown in Figure 2.13-3. The facet is shown tilted because the code is designed to handle that even though it is now used only for flat terrain. Using the small angle approximation, depression angles to the facet edge nearest the radar site are given by:

$$\gamma_1 = \frac{h_r - h_a}{G(i)}$$
$$\gamma_2 = \frac{h_t - h_a}{G - G(i)} \qquad [2.13\text{-}21]$$

where γ_1 = depression angle from radar site to edge of facet nearest radar site (facet edge *a*)
γ_2 = depression angle from target to facet edge *a*
h_a = height of facet edge *a*
h_r = height of radar site
h_t = height of target
$G(i)$ = horizontal range from radar site to facet edge *a*
G = horizontal range from radar site to target

Note that $G(i)$ can be computed from previously defined quantities.

$$G(i) = G_r(i) - \frac{1}{2} g(i) \qquad [2.13\text{-}22]$$

where $G_r(i)$ = horizontal distance from radar site to center of facet segment (Equation [2.13-15])
$g(i)$ = length of facet segment (Equation [2.13-11])

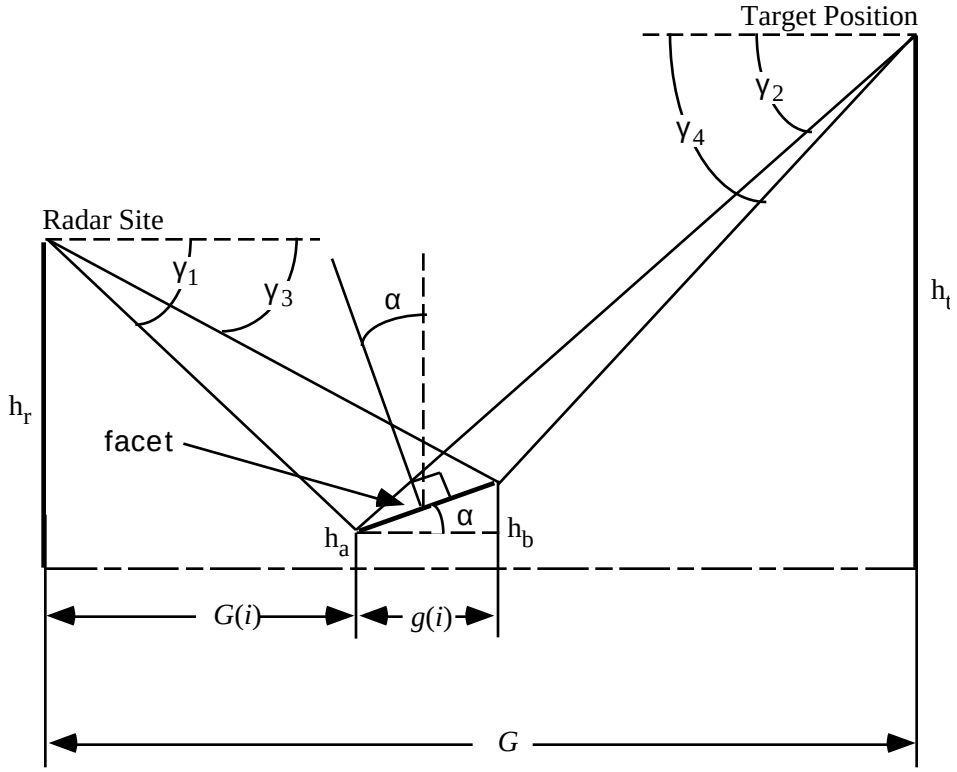

FIGURE 2.13-3. Depression Angles at Facet Edges.

Similarly, the depression angles at the facet edge nearest the target (facet edge *b*) are given by:

$$\gamma_3 = \frac{h_r - h_b}{G(i) + g(i)}$$
$$\gamma_4 = \frac{h_t - h_b}{G - (G(i) + g(i))} \qquad [2.13\text{-}23]$$

where γ_3 = depression angle from radar site to facet edge *b*
γ_4 = depression angle from target to facet edge *b*
h_b = height of facet edge *b*

(other variables defined above)

The remaining factor to consider in determining if this facet contributes a specular multipath return is α, the longitudinal tilt of the facet. In the figure, α is considered negative. Thus the "grazing" angles of the rays from the radar site and the target are given by:

$$\begin{aligned} \varphi_1 &= \gamma_1 + a \text{ (radar site to facet edge } a) \\ \varphi_2 &= \gamma_2 - a \text{ (target to facet edge } a) \\ \varphi_3 &= \gamma_3 + a \text{ (radar site to facet edge } b) \\ \varphi_4 &= \gamma_4 - a \text{ (target to facet edge } b) \end{aligned} \qquad [2.13\text{-}24]$$

(Recall that ESAMS native mode currently must use a default flat earth, so a must equal zero, but the code is designed to consider other possibilities.)

Since the angle of incidence of the radar beam must equal the angle of reflection, a point is specular if and only if the grazing angle from the radar site equals the grazing angle from the target. Thus, the facet contributes a specular multipath return if the grazing angles at edge a are equal, or if the grazing angles at edge b are equal. In fact, ESAMS does not require equality, but only that the difference between them be small compared to b0, the RMS surface roughness. It is also possible that a specular point lies on the interior of the facet. This will be true if and only if the difference between the grazing angles changes sign from edge a to edge b. Thus, the following algorithm is used:

A facet contributes a specular multipath return if and only if:

$$\begin{aligned} &|\beta_A| < \beta_0, \text{ or} \\ &|\beta_B| < \beta_0, \text{ or} \\ &\beta_A \beta_B < 0 \end{aligned} \qquad [2.13\text{-}25]$$

where $\beta_A = \varphi_1 - \varphi_2$
$\beta_B = \varphi_3 - \varphi_4$

Since facets may be tilted transversally as well as longitudinally, the azimuth of the facet return may not coincide with that of the target. The offset angle, η, is given by:

$$\eta = -\beta(\theta_{el} + \gamma_1) \qquad [2.13\text{-}26]$$

where β = transversal tilt of facet
θ_{el} = boresight elevation angle

Design Element 13-6: Diffuse Reflection Coefficient

Both specular and diffuse multipath computations will be based on models developed by D. K. Barton (Reference 10, pages 512-519). For each facet element, the amount of reflected power at the radar receiver from a completely rough surface is given by:

$$\Delta I_d = A_r^2 |\rho_0| \Delta\rho_d^2 = A_r^2 |\rho_0|^2 \left[\frac{R}{R_1 R_2}\right]^2 \frac{1}{4\pi\beta_0^2} e^{-\left(\beta/\beta_0\right)^2} \Delta S \qquad [2.13\text{-}27]$$

where: A_r = reflected field amplitude
ρ_0 = Fresnel reflection coefficient (a complex value)
β = angle between the bisector of the two reflection paths and the normal to the facet
ΔS = area of the reflecting surface over the facet
$\Delta\rho_d$ = diffuse scattering coefficient for facet
R = length of direct path from radar site to target
R1 = distance from radar site to facet
R2 = distance from facet to target

The angle β is given by:

$$\beta = \left(\frac{-\gamma_1 - \gamma_3 + \gamma_2 + \gamma_4}{4}\right) + \alpha \qquad [2.13\text{-}28]$$

However, most real surfaces are not completely rough and therefore give rise to partially diffuse and partially specular reflection. The relative magnitudes of the specular and diffuse scattering coefficients vary over the reflecting surface, and as a result the diffuse scattering coefficient is multiplied by a roughness factor:

$$F_d^2 = \sqrt{\left(1-\rho_{s_1}^2\right)\left(1-\rho_{s_2}^2\right)} \qquad [2.13\text{-}29]$$

where: ρ_{s_1} and ρ_{s_2} = RMS scattering coefficients due to roughness

The RMS scattering coefficients are given by (Reference 10, page 293):

$$\rho_{s_j} = e^{-2\left(\frac{2\pi}{\lambda}\beta_0 \sin\psi_j\right)^2} \quad j=1,\ 2 \qquad [2.13\text{-}30]$$

where: $\Psi 1$ and $\Psi 2$ = reflected grazing angles to the radar site and target at the center of the ground line segment intersecting the facet

The grazing angles at the center of the facet segment are computed analogously to those at the facet edges (see Equations [2.13-18] through [2.13-20]). Using the fact that small angles are approximately equal to their tangents, the angles are given by:

$$\psi_1 = \frac{h_r - h_c}{G_r(i)} - \alpha$$

$$\psi_2 = \frac{h_t - h_c}{G - G_r(i)} + \alpha \qquad [2.13\text{-}31]$$

where h_t = height of target
h_r = height of radar site
h_c = height at center of facet segment
$G_r(i)$ = ground distance to center of facet segment

G = ground distance from radar site to target
α = longitudinal tilt of facet

Many of these variables are shown in Figure 2.13-3. Note that h_c is simply the average of h_a and h_b as shown in the figure.

From Reference 10, page 292, the complex-valued Fresnel coefficient is:

$$\rho_0 = \frac{\varepsilon_r \sin\Psi - \sqrt{\left(\varepsilon_r - cos^2\,\Psi\right)}}{\varepsilon_r \sin\Psi + \sqrt{\left(\varepsilon_r - \cos^2\Psi\right)}} \qquad [2.13\text{-}32]$$

for a vertical polarization and

$$\rho_0 = \frac{\sin\Psi - \sqrt{\left(\varepsilon_r - cos^2\,\Psi\right)}}{\sin\Psi + \sqrt{\left(\varepsilon_r - \cos^2\Psi\right)}} \qquad [2.13\text{-}33]$$

for a horizontal polarization

where: ε_r = complex-valued dielectric constant for the surface
Ψ = incident grazing angle

The width of a reflecting surface, W_i, generated by the site-target geometry is given by (see Reference 9, pages 256-259):

$$W_i = \left[\frac{G_s(i)\left(R - G_s(i)\right)}{R}\right]\left[\frac{h_r}{G_s(i)} + \frac{h_r}{R - G_s(i)}\right]\sqrt{\beta_0^2 - \frac{1}{4}\left(\frac{h_r}{G_s(i)} - \frac{h_r}{R - G_s(i)}\right)^2} \qquad [2.13\text{-}34]$$

where: $G_s(i)$ = distance along the ground line from the radar site to the ith facet element
R = distance from radar to target
R_1 = distance from radar to facet
R_2 = distance from facet to target
h_r = height of radar site
β_0 = RMS slope of surface irregularities

Assuming small grazing angles, the following approximation can be made:

$$G_s(i) \approx R_1, \quad R - G_s(i) \approx R_2, \quad \frac{h_r}{G_s(i)} = tan\,\Psi_1 \approx \Psi_1, \quad \frac{h_t}{R - G_s(i)} = tan\,\Psi_2 \approx \Psi_2 \qquad [2.13\text{-}35]$$

Making these substitutions gives:

$$W_i = \frac{R_1 + R_2}{R}\left(\psi_1 + \psi_2\right)\sqrt{\beta_0^2 - \frac{1}{4}\left(\psi_1 - \psi_2\right)^2} \qquad [2.13\text{-}36]$$

Assuming that the second term under the radical is negligible and multiplying this width by the facet segment length, the area of the reflecting surface over the facet is given by:

$$\Delta S \approx \beta_0 \left(\frac{R_1 R_2}{R}\right)\left(\Psi_1 + \Psi_2\right) g(i) \qquad [2.13\text{-}37]$$

Using the formula for $\Delta\rho_d^2$ implicit in Equation [2.13-23], multiplying by F_d^2 from Equation [2.13-27], and substituting ΔS as defined in Equation [2.13-37], the diffuse portion of the reflection coefficient is given by:

$$\Delta\rho_d^2 = \left[\frac{R}{R_1 R_2}\right]\left[\frac{F_d^2}{4\sqrt{\pi}\beta_0}\right] e^{-\left(\frac{\beta}{\beta_0}\right)^2} \left(\Psi_1 + \Psi_2\right) g(i) \qquad [2.13\text{-}38]$$

Design Element 13-7: Specular Reflection Coefficient

It is generally accepted that specular reflection arises from the first Fresnel zone. The first Fresnel zone is the region from which path length deviations from direct reflection are less than one half of the transmitted wavelength. The resulting area forms an ellipse whose major axis lies along the site-to-target ground line with length given by (see Reference 12, page 22):

$$l = G\left[1 + \frac{2\delta}{\lambda}\right]^{\frac{1}{2}} \left[1 + \frac{\left(h_r + h_t\right)^2}{\lambda G}\right]^{-1} \qquad [2.13\text{-}39]$$

where:
- G = ground range from radar site to target
- λ = transmitted wavelength
- δ = difference between direct and indirect path lengths
- h_r = height of radar site
- h_t = height of target

The specular reflection coefficient ρ is the product of three factors (Reference 10, page 291):

$$\rho = \rho_v \rho_s \rho_0 \qquad [2.13\text{-}40]$$

where:
- ρ_v = vegetation factor
- ρ_s = RMS scattering due to roughness
- ρ_0 = Fresnel reflection coefficient

ESAMS assumes that ρ_v=1 (light vegetation). The Fresnel reflection coefficient, , is defined in Equation [2.13-28] or Equation [2.13-29]. The scattering due to roughness is defined in Equation [2.13-26] (note that $\psi_1=\psi_2=\psi(i)$, and hence, $\rho_{s1}=\rho_{s2}=\rho_s(i)$ for specular returns). Thus, the specular reflection coefficient for each facet that intersects the major axis of the first Fresnel zone is given by:

$$\rho = \rho_0 \rho_s \frac{g_s(i)}{l} \qquad [2.13\text{-}41]$$

where: $\frac{g_s(i)}{l}$ = gives the fraction of the major axis lying in that facet

Summing over all contributing facets and including a factor to account for a phase shift due to the path length difference, δ, gives ρ as follows:

$$\rho = e^{-\frac{2\pi i}{\lambda}\delta} \sum_{i=1}^{N} \rho_{0_i} \rho_{s_i} g_{0_i} \qquad [2.13\text{-}42]$$

where: N = total number of participating facets

Design Element 13-8: Multipath Signals

Once the participating terrain facets have been identified and their specular and diffuse reflection coefficients have been computed, the sum and difference channel signals corresponding to the composite multipath effect will be computed. This involves completing the radar range equation using antenna gain factors in the direction of the target and each participating facet element.

The directional gains of the antenna response are functions of the object pointing unit vector ($\vec{x}$ for the target and $\vec{f}_i$ for the i^{th} facet element) and boresight pointing angles θ_{az} and θ_{el}. The sum channel gains can be denoted as:

$$\begin{aligned} G_{T\Sigma} &= F_\Sigma(\vec{x}, \theta_{az}, \theta_{el}) \\ G_{F_i\Sigma} &= F_\Sigma(\vec{f}_i, \theta_{az}, \theta_{el}) \end{aligned} \qquad [2.13\text{-}43]$$

Difference channel gains are denoted:

$$\begin{aligned} G_{TAZ} &= F_{AZ}(\vec{x}, \theta_{az}, \theta_{el}) \\ G_{F_iAZ} &= F_{AZ}(\vec{f}_i, \theta_{az}, \theta_{el}) \\ G_{TEL} &= F_{EL}(\vec{x}, \theta_{az}, \theta_{el}) \\ G_{F_iEL} &= F_{EL}(\vec{f}_i, \theta_{az}, \theta_{el}) \end{aligned} \qquad [2.13\text{-}44]$$

See Section 2.20 for a complete description of the antenna gain function.

Since the specular component is the result of a coherent reflection, the specular reflection coefficient ρ completely defines amplitude attenuation and phase shift. Determining the diffuse component, however, is a stochastic process. Hence, the diffuse reflection gain will be defined as a distribution about a specular bias. This approach will use the Ricean distribution which characterizes a deterministic signal in the presence of noise (see Reference 10, page 61) to generate a composite multipath reflection coefficient, ρ_i for each participating facet element.

The complex-valued sum and difference channel composite multipath voltages over all participating facet elements are given by:

$$V_\Sigma = \frac{\lambda F_{MTI} \sqrt{P_T \sum_{i=1}^{N} \rho_i \sqrt{\sigma_i} G_{T\Sigma}^2 G_{F_i\Sigma}^2}}{2\sqrt{\pi^3} R^2 L}$$

$$V_{AZ} = \frac{\lambda F_{MTI} \sqrt{P_T \sum_{i=1}^{N} \rho_i \sqrt{\sigma_i} G_{T\Sigma}^2 G_{F_iAZ}^2}}{2\sqrt{\pi^3} R^2 L} \qquad [2.13\text{-}45]$$

$$V_{EL} = \frac{\lambda F_{MTI} \sqrt{P_T \sum_{i=1}^{N} \rho_i \sqrt{\sigma_i} G_{T\Sigma}^2 G_{F_iEL}^2}}{2\sqrt{\pi^3} R^2 L}$$

where:
- ρ_i = composite reflection coefficient
- G = directional gains defined in Equations [2.3-43] and [2.3-44]
- σ_i = target signature as viewed from the i^{th} facet element
- P_T = transmitted power
- F_{MTI} = Moving Target Indicator (MTI) attenuation factor as a function of the apparent Doppler frequency of the multipath signal
- L = receiver processing loss factor

Design Element 13-9: Doppler Centroid

To facilitate MTI processing (see Section 2.23), a centroid value representing the apparent Doppler shift of the composite multipath signal will be computed. This involves calculating the component of the target velocity in the direction of each facet element:

$$v_i = \frac{\vec{f}_{T_i} \dot{x}}{\left|\vec{f}_{T_i}\right|} \qquad [2.13\text{-}46]$$

where:
- $\vec{f}_{T_i}$ = facet position vector relative to the target
- $\dot{x}$ = target velocity vector

The Doppler shift for a particular facet element is then given by:

$$f_{d_i} = \frac{-2v_i}{\lambda} \qquad [2.13\text{-}47]$$

The Doppler shift at each facet element is weighted by the modulus of the sum channel voltage. The Doppler centroid is formed as follows:

$$\bar{f}_d = \frac{\sum_{i=1}^{N} f_{d_i} \left| \rho_i \sqrt{\sigma_i} G_{T\Sigma}^2 G_{F_i\Sigma}^2 \right|}{\sum_{i=1}^{N} \left| \rho_i \sqrt{\sigma_i} G_{T\Sigma}^2 G_{F_i\Sigma}^2 \right|} \qquad [2.13\text{-}48]$$

GRACE Multipath Design

The GRACE multipath implementation will utilize Site Mask data, which is a much condensed representation of the terrain-form data. The Site Mask terrain data are given in terms of a set of radials (normally every 0.5 degree) about the radar site; for each radial there is a set of terrain patches capable of being illuminated by the radar. Each illumination patch is specified by four values:

1. The ground range (great circle arc length at mean sea level) from the radar site to the start of the illumination patch (or re-illumination point following a mask point).
2. The ground range to the mask point at the end of the illumination patch.
3. The altitude of this mask point.
4. The altitude of the point midway in ground range between the start and the end of the illumination patch.

The GRACE multipath implementation will also utilize the Environmental Characteristics Package to obtain values of the magnitude and phase shift of the ground reflectivity. Default values will be set at 0.5 for reflectivity and 180 degrees for phase shift for all terrain cover, so that in this respect there will be no difference between different terrain covers. However, this can be changed when adequate data become available to insert into the Environmental Characteristics Package.

The GRACE multipath implementation will not filter multipath signals to eliminate those contributions which would fall outside the range gate of the tracking radar. Similarly, only the effects on angle and Doppler tracking will be implemented. In addition, only contributions from the Site Mask radial nearest the bearing of the target will be computed. It will be implicit in the condensed terrain representation in the Site Mask data, that no effect of terrain tilt tangential to a radial will be included in the multipath calculations.

Design Element 13-10: Terrain Representation

The terrain area is divided into a series of radial sectors whose angular extent is given by:

$$\Delta\theta = \frac{2\pi}{N_R} \qquad [2.13\text{-}49]$$

where *NR* = the user-specified number of radials

For the purpose of data identification, each radial is sequentially numbered starting at the first radial clockwise from due north, and proceeding clockwise through all N_R radials. To access the appropriate site mask data, the radial segment in which the target falls must be determined. The target bearing from true north is given by:

$$\alpha = tan^{-1}\left[\frac{x_t - x_r}{y_t - y_r}\right] \qquad [2.13\text{-}50]$$

where (x_r,y_r,z_r) and (x_t,y_t,z_t) are the coordinates of the radar site and the target, respectively.

Thus, the radial segment that will supply the appropriate masking data is given by:

$$n_R = \left\| \frac{\alpha}{\Delta\theta} \right\| + 1 \qquad [2.13\text{-}51]$$

where || || denotes the greatest integer function

The key geometrical features of the radar site, target and terrain relationships for a single illumination patch on the appropriate radial are shown in Figure 2.13-4. The illumination patches will be referred to as facets (NOTE: the use of the term “facet” simplifies notation, but does not imply the use of the facet structure from the native multipath implementation, nor does it refer to the triangular representation of the digital terrain data).

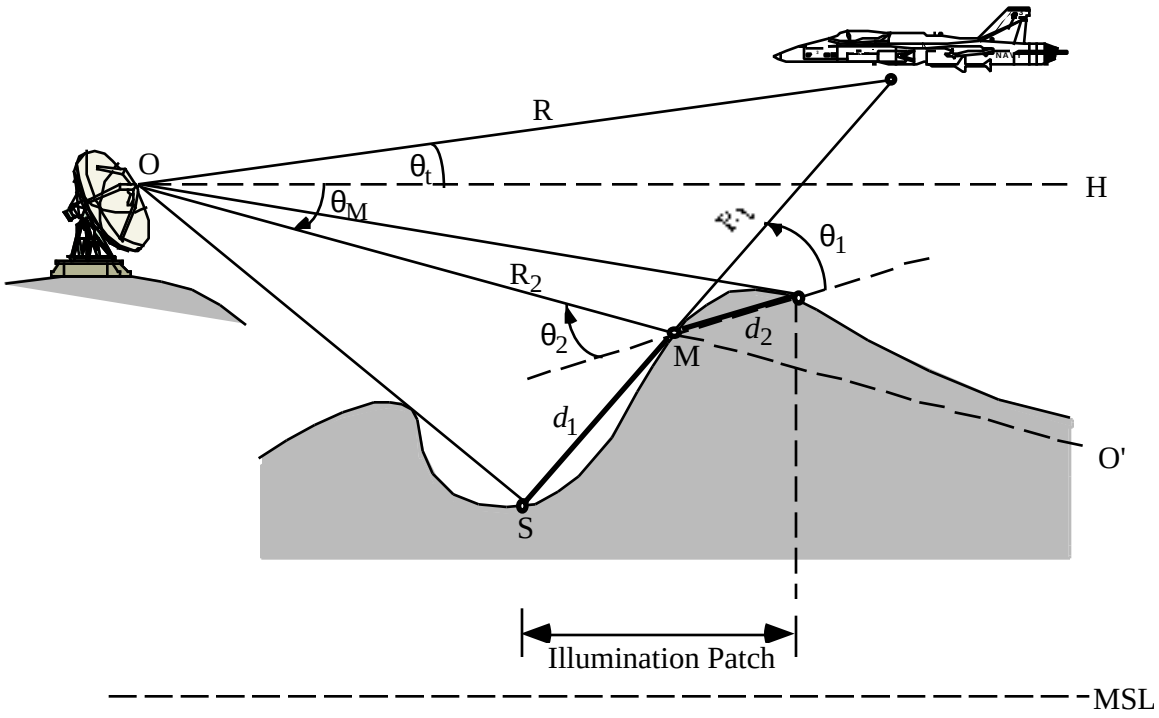

FIGURE 2.13-4. Radar, Terrain and Target Geometry.

As shown in Figure 2.13-4, terrain facets are contiguous segments of terrain marked by a starting point *S*, a midpoint *M*, and an endpoint *E*. These three points, and the two straight line segments joining them, represent a very condensed view of the actual terrain between *S* and *M* and between *M* and *E*. This data will be stored as part of the pre-computed Site Mask data (see Section 2.11).

The entire multipath contribution over an illuminated facet is considered to result from the length d_2 between the facet midpoint *M* and the masked point *E* shown in Figure 2.13-4. Reflection patterns are computed as a function of the grazing angles θ_2 and θ_1 of rays from the radar and the target, respectively, to the facet midpoint *M*. To find these grazing angles, the law of cosines can be used to express the relationship between the two grazing angles and known lengths as follows:

$$cos(\pi - \theta_2) = \frac{R_2^2 + d_2^2 - R^2}{2R_2 d_2} \qquad [2.13\text{-}52]$$

and

$$cos(\pi - \theta_1 - \theta_2) = \frac{R_1^2 + R_2^2 - R^2}{2R_1 R_2} \qquad [2.13\text{-}53]$$

where R = line-of-sight distance between the radar site and the facet midpoint *M* (available directly from site mask data)

d_2 = length of the ground line between the facet midpoint *M* and the masking point *E* (available directly from site mask data)

R = line-of-sight range from the radar site to the target

R_1 = range from the facet midpoint to the target

The range *R* can be computed from the site and target coordinates.

$$R = \sqrt{(x_t - x_r)^2 + (y_t - y_r)^2 + (z_t - z_r)^2} \qquad [2.13\text{-}54]$$

The range R_1 is given by the law of cosines as:

$$R_1 = \sqrt{R^2 + R_2^2 - 2RR_2\, cos(\theta_t - \theta_M)} \qquad [2.13\text{-}55]$$

where θ_t = target elevation angle

θ_M = elevation of the facet midpoint (available directly from site mask data)

The target elevation angle θ_t is computed as:

$$\theta_t = sin^{-1}\left[\frac{z_t - z_r}{R}\right] \qquad [2.13\text{-}56]$$

The reflection pattern also depends on the effective radial length d_e and effective scattering area A_e of the facet. The effective facet length is computed as the geometrical average of the length d_2 projected in the direction of the radar site and the target.

$$d_e = d_2 \sqrt{\sin\theta_2 \sin\theta_1} \qquad [2.13\text{-}57]$$

The effective scattering area is:

$$A_e = d_e R_2 \sin\varphi_B \qquad [2.13\text{-}58]$$

where θ_B = half-power beamwidth of the radar antenna

Design Element 13-11: Specular Reflection Pattern

The voltage for a rectangular aperture of width *w* and height *h* is given by Barton (Reference 10, page 150) as follows:

$$f(\theta,\varphi) = \frac{\sin\left(\frac{\pi w}{\lambda}\sin\theta\cos\varphi\right)}{\frac{\pi w}{\lambda}\sin\theta\cos\varphi} \; \frac{\sin\left(\frac{\pi h}{\lambda}\sin\theta\cos\varphi\right)}{\frac{\pi h}{\lambda}\sin\theta\cos\varphi} \qquad [2.13\text{-}59]$$

The power pattern $G(\theta)$ is defined to be $f^2(\theta,0)$ with $w = d_e$; hence, it can be written as follows:

$$G(\theta) = \left[\frac{\sin\left(\frac{\pi d_e}{\lambda}\sin\theta\right)}{\frac{\pi d_e}{\lambda}\sin\theta}\right]^2 \qquad [2.13\text{-}60]$$

Rectangular plate reflection depends on the direction of the illumination. Figure 2.13-5 shows the reflection pattern of a rectangular plate with the main lobe of reflection aligned along the specular ray.

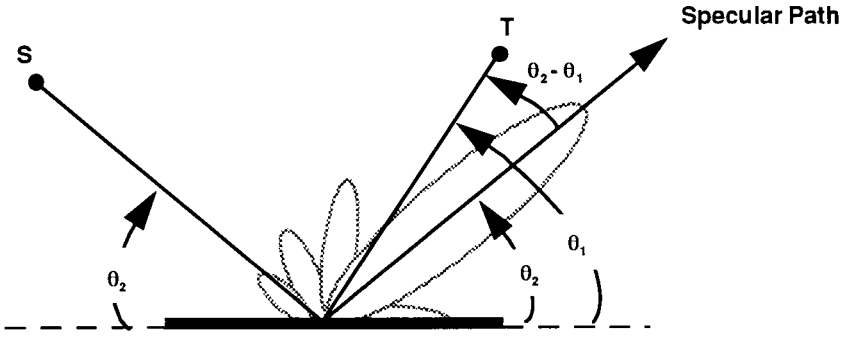

FIGURE 2.13-5. Specular Reflection Pattern.

The angle of the target off the specular path is given by the difference in grazing angles, hence the power reflected in the direction of the target can be written as:

$$G(\theta_2 - \theta_1) = \left[\frac{\sin\left(\frac{\pi d_e}{\lambda} \sin(\theta_2 - \theta_1)\right)}{\frac{\pi d_e}{\lambda} \sin(\theta_2 - \theta_1)} \right]^2 \qquad [2.13\text{-}61]$$

$G(\theta_2 - \theta_1)$ can also be referred to in terms of the sinc function where $sinc(x) = sin(x)/x$. Thus:

$$G(\theta_2 - \theta_1) = sinc^2\left(\frac{\pi d_e}{\lambda} \sin(\theta_2 - \theta_1)\right) \qquad [2.13\text{-}62]$$

Design Element 13-12: Multipath Voltage

Each radial may yield several contributing facets. For each of these facets along the Site Mask radial nearest to the bearing of the target, a contribution to the sum and difference channel voltages will be computed. For each facet, the sum and difference channel voltages are derived from the bistatic radar range equation as:

$$V_\Sigma = \sqrt{\left[\frac{P_T \lambda^2}{(4\pi)^3 R^2 L}\right]\left[\frac{\sigma A_e}{2\pi R_1^2 R_2^2}\right]} \times \sqrt{\rho_{dif} + \rho_{spec} \frac{4\pi A_e}{\lambda^2} sinc^2\left(\frac{d_e \sin(\theta_2 - \theta_1)}{\lambda}\right)} \left[G_{T\Sigma} G_{F\Sigma}\right] e^{\frac{j2\pi\delta_R}{\lambda}}$$

$$V_{AZ} = \sqrt{\left[\frac{P_T \lambda^2}{(4\pi)^3 R^2 L}\right]\left[\frac{\sigma A_e}{2\pi R_1^2 R_2^2}\right]} \times \sqrt{\rho_{dif} + \rho_{spec} \frac{4\pi A_e}{\lambda^2} sinc^2\left(\frac{d_e \sin(\theta_2 - \theta_1)}{\lambda}\right)} \left[G_{T\Sigma} G_{FAZ} + G_{F\Sigma} G_{TAZ}\right] e^{\frac{j2\pi\delta_R}{\lambda}} \qquad [2.13\text{-}63]$$

$$V_{EL} = \sqrt{\left[\frac{P_T \lambda^2}{(4\pi)^3 R^2 L}\right]\left[\frac{\sigma A_e}{2\pi R_1^2 R_2^2}\right]} \times \sqrt{\rho_{dif} + \rho_{spec} \frac{4\pi A_e}{\lambda^2} sinc^2\left(\frac{d_e \sin(\theta_2 - \theta_1)}{\lambda}\right)} \left[G_{T\Sigma} G_{FEL} + G_{F\Sigma} G_{TEL}\right] e^{\frac{j2\pi\delta_R}{\lambda}}$$

where:
- L = receiver loss figure
- P_T = transmitted power
- λ = radar wavelength
- σ = bistatic RCS of the target with respect to the radar and facet
- ρ_{dif} and ρ_{spec} = diffuse and specular reflection coefficients (available directly from the terrain data base)
- R, R_1, R_2, A_e, and d_e defined above
- δ_R = difference between the direct and multipath paths to the target:

$$\delta_R = mod(R_1 + R_2 - R, \lambda) \qquad [2.13\text{-}64]$$

The directional gains of the antenna are functions of object pointing vector ($\vec{x}$ for the target and $\vec{f}_i$ for the i^{th} facet element) and boresight pointing angles θ_{az} and θ_{el}. The bearing of the facets is assume to be α, the same as the target bearing. If θ_M denotes the elevation of the facet midpoint, then the components of the unit vector pointing from the radar site to the facet midpoint are:

$$\begin{aligned} r_x &= sin\alpha cos\theta_M \\ r_y &= cos\alpha cos\theta_M \\ r_z &= sin\theta_M \end{aligned} \qquad [2.13\text{-}65]$$

The vector pointing from the radar site to the facet midpoint is then given by:

$$\vec{R}_2 = R_2\left(r_x\hat{i} + r_y\hat{j} + r_z\hat{k}\right) \qquad [2.13\text{-}66]$$

The vector pointing from the radar site to the target is:

$$\vec{x} = \left(x_t - x_s\right)\hat{i} + \left(y_t - y_s\right)\hat{j} + \left(z_t + z_s\right)\hat{k} \qquad [2.13\text{-}67]$$

and the vector pointing from the facet to the target is:

$$\vec{f} = \vec{R} - \vec{R}_2 = \left(x_t - x_s - R_2 r_x\right)\hat{i} + \left(y_t - y_s - R_2 r_y\right)\hat{j} + \left(z_t - z_s - R_2 r_z\right)\hat{k} \qquad [2.13\text{-}68]$$

The sum channel antenna gains can be denoted as:

$$\begin{aligned} G_{T\Sigma} &= F_\Sigma\left(\vec{x}, \theta_{az}, \theta_{el}\right) \\ G_{F\Sigma} &= F_\Sigma\left(\vec{f}, \theta_{az}, \theta_{el}\right) \end{aligned} \qquad [2.13\text{-}69]$$

and the difference channel gains are:

$$\begin{aligned} G_{TAZ} &= F_{AZ}\left(\vec{x}, \theta_{az}, \theta_{el}\right) \\ G_{FAZ} &= F_{AZ}\left(\vec{f}, \theta_{az}, \theta_{el}\right) \\ G_{TEL} &= F_{EL}\left(\vec{x}, \theta_{az}, \theta_{el}\right) \\ G_{FEL} &= F_{EL}\left(\vec{f}, \theta_{az}, \theta_{el}\right) \end{aligned} \qquad [2.13\text{-}70]$$

where F_{AZ} and F_{EL} are the sum and difference antenna gain functions (see Section 2.20, Antenna Gain).

Design Element 13-13: Doppler Centroid

To facilitate MTI processing (see Section 2.23), a centroid value representing the apparent Doppler shift of the composite multipath signal will be computed. The Doppler centroid from the multipath will be accumulated as a weighted sum:

$$\bar{f}_d = \frac{\sum_{i=1}^{N} \left(-\frac{2\vec{V}_T \quad \vec{R}_{1_i}}{\lambda R_{1_i}} \right) \left| V_{\Sigma_i} \right|}{\sum_{i=1}^{N} \left| V_{\Sigma_i} \right|} \qquad [2.13\text{-}71]$$

where: $\vec{V}_T$ = velocity of the target
$\vec{R}_1$ = vector of length R_1 directed from the facet to the target

2.13.3 Multipath Functional Element Software Design

Section 2.13.3 is divided into two parts containing descriptions of the functional element software design for both the native and GRACE multipath implementations.

Native Multipath Software Design

Seven subroutines are required to implement the native multipath design outlined in Section 2.13.2. The call hierarchy within the RF sensor model is also given. The next part of this section presents the logical flow charts of the subroutines comprising the functional element implementation and describes the important operations contained in the flow chart blocks. Finally, the last part of the section on native multipath software design discusses the input and output data variables associated with each subroutine.

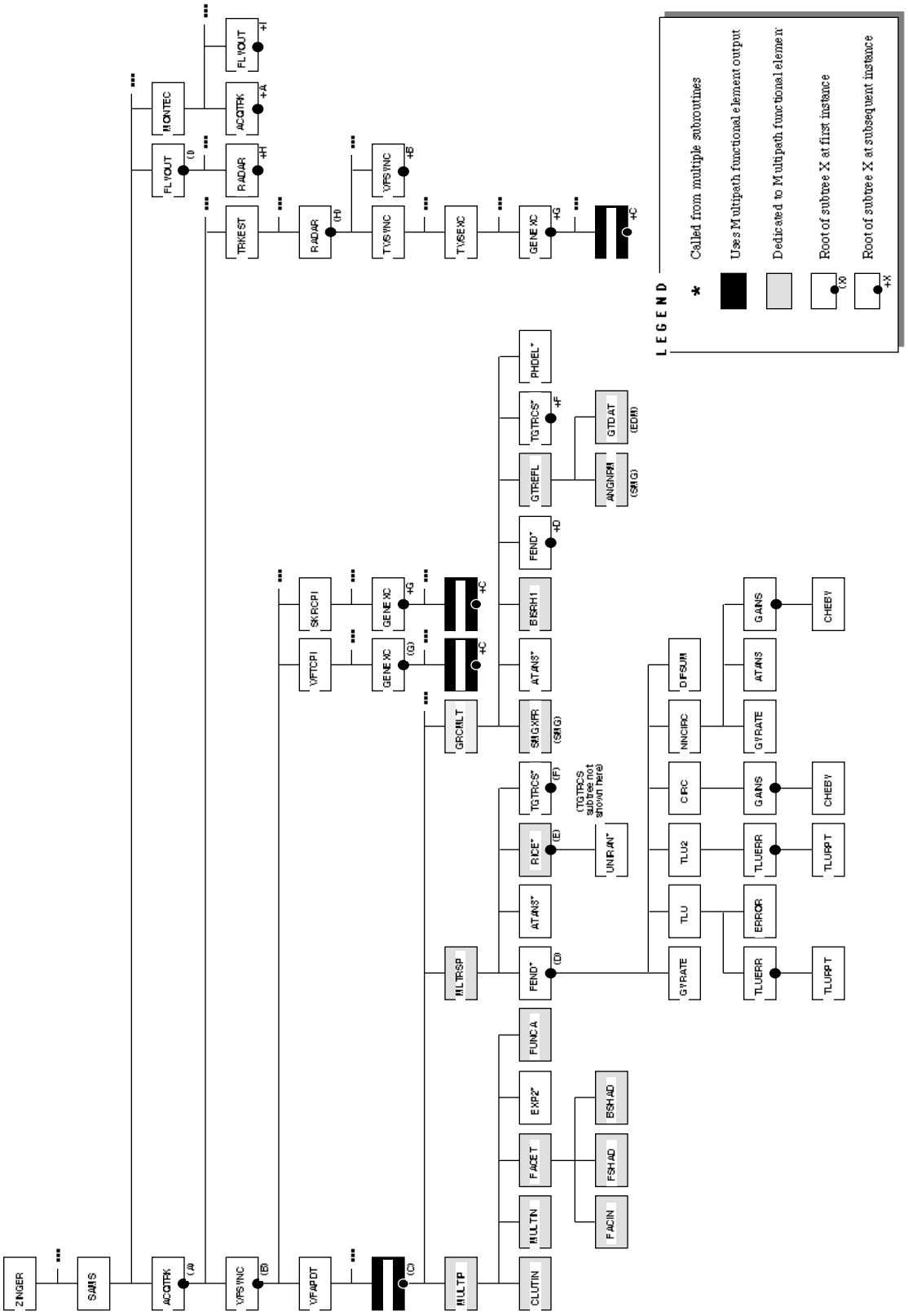

FIGURE 2.13-6. Native Multipath Subroutine Call Hierarchy Diagram.

Native Multipath Subroutine Design

The subroutine call hierarchy diagram for the native multipath implementation is shown in Figure 2.13-6. This diagram shows the calling sequence of the native multipath functional element within the entire ESAMS model structure. The seven subroutines which implement the functional element appear in shaded blocks. Subroutines which use the native multipath functional element output appear in filled in blocks. A brief description of each subroutine appears in Table 2.13-2.

TABLE 2.13-2. Native Multipath Subroutine Descriptions.

MULTIP	Calculates the specular and diffuse multipath reflection coefficients.
MULTIN	Initialize variables associated with multipath calculations.
FACET	Determines the participating facets given radar site and target position geometry.
FACIN	Loads and initialize facet data.
MLTRSP	Calculates the sum and difference channel voltages due to multipath effects.

Native Multipath Logic Flow

The block diagram in Figure 2.13-7 shows the functions that determine the impact of native multipath effects on target tracking and acquisition. Each block contains a specific function and the subroutine in which that function will occur. The names of the subroutines are in parentheses.

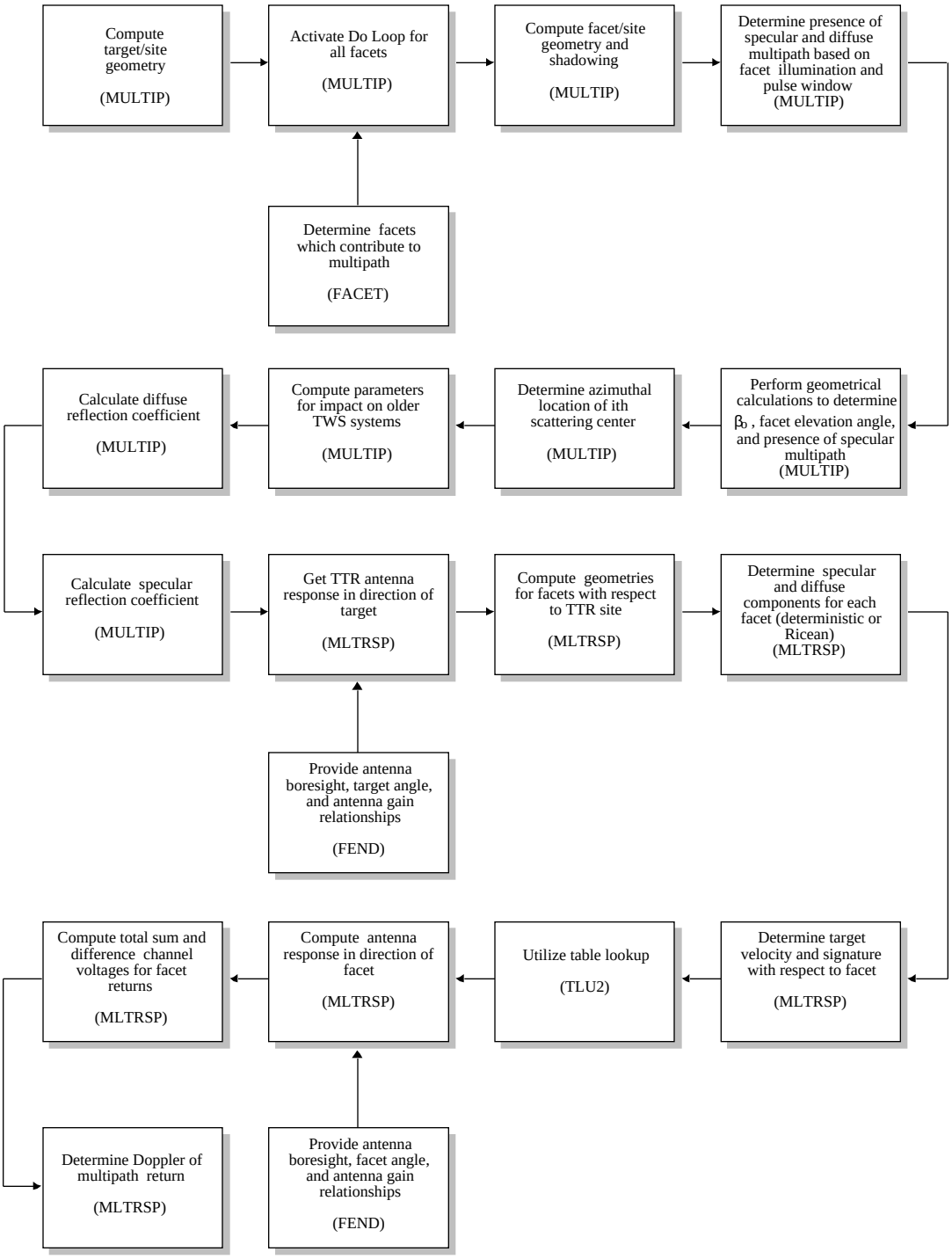

FIGURE 2.13-7. Native Multipath Block Diagram.

Figure 2.13-8 shows the logic flow chart for subroutine MULTIP. The numbered blocks in the flow chart are discussed below.

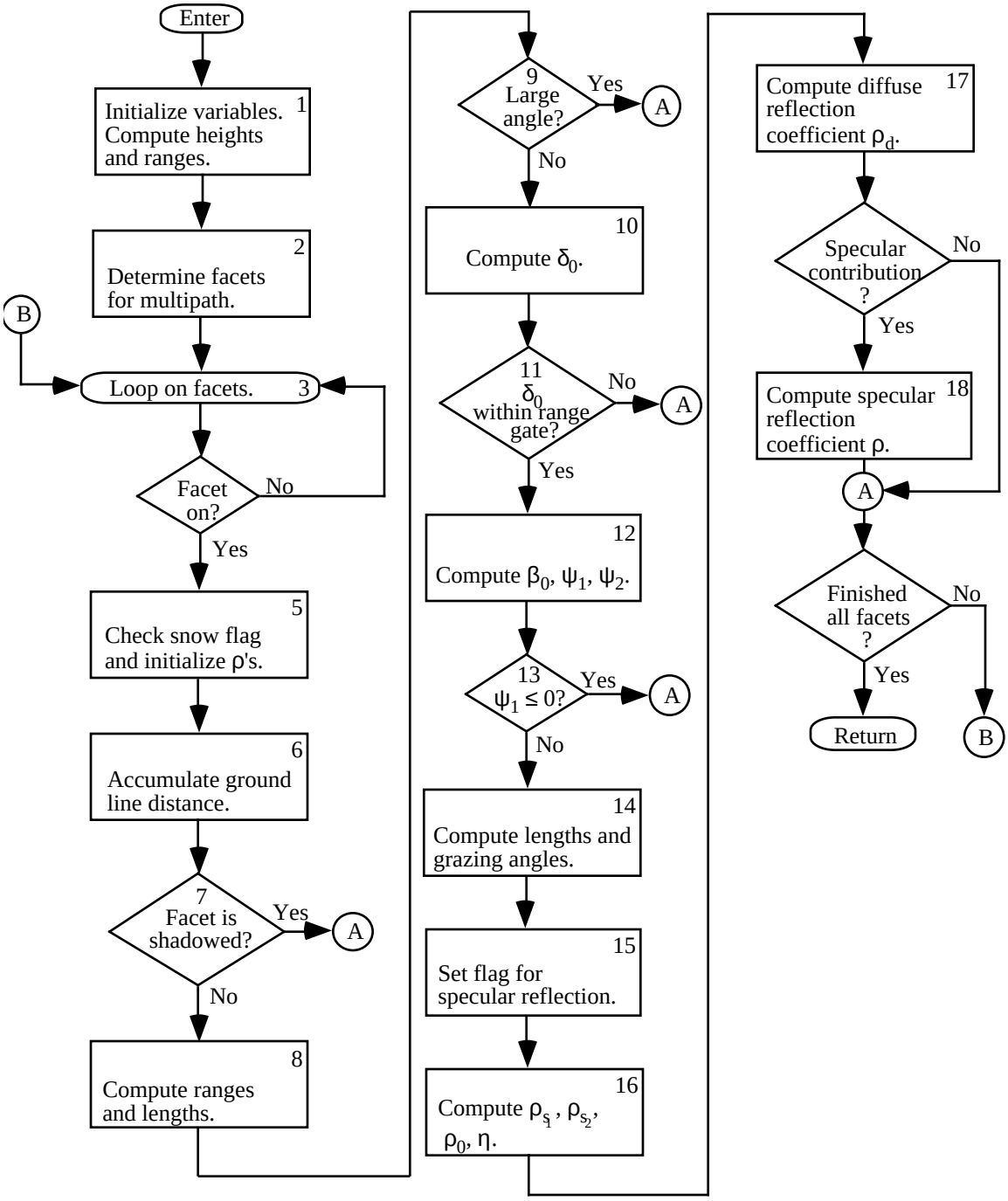

FIGURE 2.13-8. Subroutine MULTIP Logic Flow Chart.

Block 1. The first step initialize all variables used in the multipath computations. Calls to CLUTTIN and MULTIN are executed to initialize clutter and multipath electronic constants. Radar site and target geometry is initialized by computing site and target altitudes relative to a global reference plane and line-of-site ranges are computed. Also at this point, a flag is set indicating wet or dry terrain.

Block 2. This block represents a call to subroutine FACET which determines which facet elements will be included in the multipath calculations as a result of the site-target geometry. Details of this process are shown in Figure 2.13-10.

Block 3. This step marks the beginning of a loop to process all participating facet elements. At this point variables representing site-to-target ground line distance and the length of the Fresnel zones across each facet element are initialized.

Block 4. A decision is made as to whether or not the facet is turned on by checking the terrain type flag IFACET(4,I). If this terrain type has been set to zero, then no multipath contribution from this facet will be computed.

Block 5. If snow conditions have been indicated, then the terrain type is set to "snow."

Reflection coefficients are initialized to zero. The diffuse (noncoherent) reflection coefficient is a real number while the specular (coherent) reflection coefficient is a complex number.

Block 6. This step accumulates the ground line distance from the site to the center of the segment crossing the current facet. See Equation [2.13-15].

Block 7. Facet shadowing is checked at this step by examining the shadow flag set during the execution of subroutine FACET. Note again that because native mode is not currently mated to terrain, no facets will be shadowed.

Block 8. The distance from the target to the center of the ground line segment on the current facet is computed as in Equation [2.13-16], and the altitude of the radar site above the facet is computed by subtraction.

Block 9. This step determines if the elevation angle to the facet is more than twenty beamwidths off boresight of the radar antenna. If so, the current facet is passed over since multipath contribution would be negligible.

Block 10. The path length difference between the direct and indirect return paths is computed according to Equations [2.13-14] through [2.13-18].

Block 11. A check is made to determine whether or not the indirect pulse arrives within the range gate time interval. If not, the current facet is passed over for computation.

Block 12. Geometric quantities representing the RMS slope of the surface irregularities β_0 and the grazing angles Ψ_1 and Ψ_2 are computed at this step. The RMS slope β_0, is computed using Equation [2.13-20], and Ψ_1 and Ψ_2 are given by Equation [2.13-31].

Block 13. A check is made to determine if the facet is self-shadowed, meaning that the surface is hidden (tilted away) from the radar site. If Ψ_1 is less than zero, then the facet is self shadowed and is not considered for further multipath computation.

Block 14. This step involves the calculation of quantities associated with the determination of a specular condition. The length l of the first Fresnel zone across the current facet is computed from Equation [2.13-39]. Grazing angles at the facet edges are then computed according to Equations [2.13-21] through [2.13-24]. Checks are made to account for situations when the target or the radar is above the current facet. In this case, the grazing angle is set to a very large number to ensure that the grazing angles are not within β_0 of each other.

Block 15. Algorithm [2.13-25] is used to determine if this facet contributes a specular multipath return. If any one of the three conditions are met, then a Boolean variable is set to true indicating that the facet supports specular reflection.

Block 16. This step computes the RMS scattering coefficients ρ_{s_1} and ρ_{s_2} according to Equation [2.13-30].

The complex-valued Fresnel coefficient ρ_0 is computed depending on the polarization of the radar according to Equations [2.13-32] and [2.13-33].

The apparent azimuthal location of the current facet η_i is computed using Equation [2.13-26] and stored for use in subroutine MLTRSP.

Block 17. The diffuse reflection coefficient is accumulated next. This involves computing the factor F_d^2 according to Equation [2.13-29], the diffuse power coefficient for the current facet given by Equation [2.13-38] and then storing the square root of the coefficient, ρ_d.

Block 18. After checking the specular condition computed in Block 15, the complex-valued specular reflection coefficient is computed as the accumulation sum in Equation [2.13-42].

Figure 2.13-9 shows the logic flow chart for subroutine MULTIN. The numbered blocks in the flow chart are discussed below.

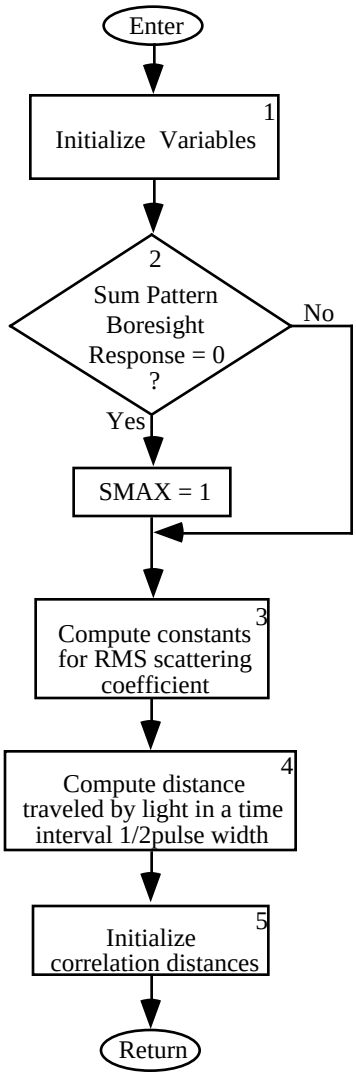

FIGURE 2.13-9. Subroutine MULTIN Logic Flow Chart.

Block 1. Variables representing the diffuse and specular reflection coefficients, the apparent azimuthal location of the facet, and the site-to-facet depression angle are initialized to zero.

Block 2. The absolute sum pattern boresight response is checked for nonzero response. If the response is zero, then it is reset to unity to avoid division by zero.

Block 3. Numerical constants used in the RMS scattering coefficients given by Equation [2.13-30] are computed.

Block 4. The distance traveled by light in a time interval equal to one-half of a pulse width is computed to determine whether the multipath pulse arrives within the range gate.

Block 5. Correlation distances for the nine terrain types are initialized by arbitrarily setting them all equal to 10.0.

Figure 2.13-10 shows the logic flow chart for subroutine FACET. The numbered blocks in the flow chart are discussed below.

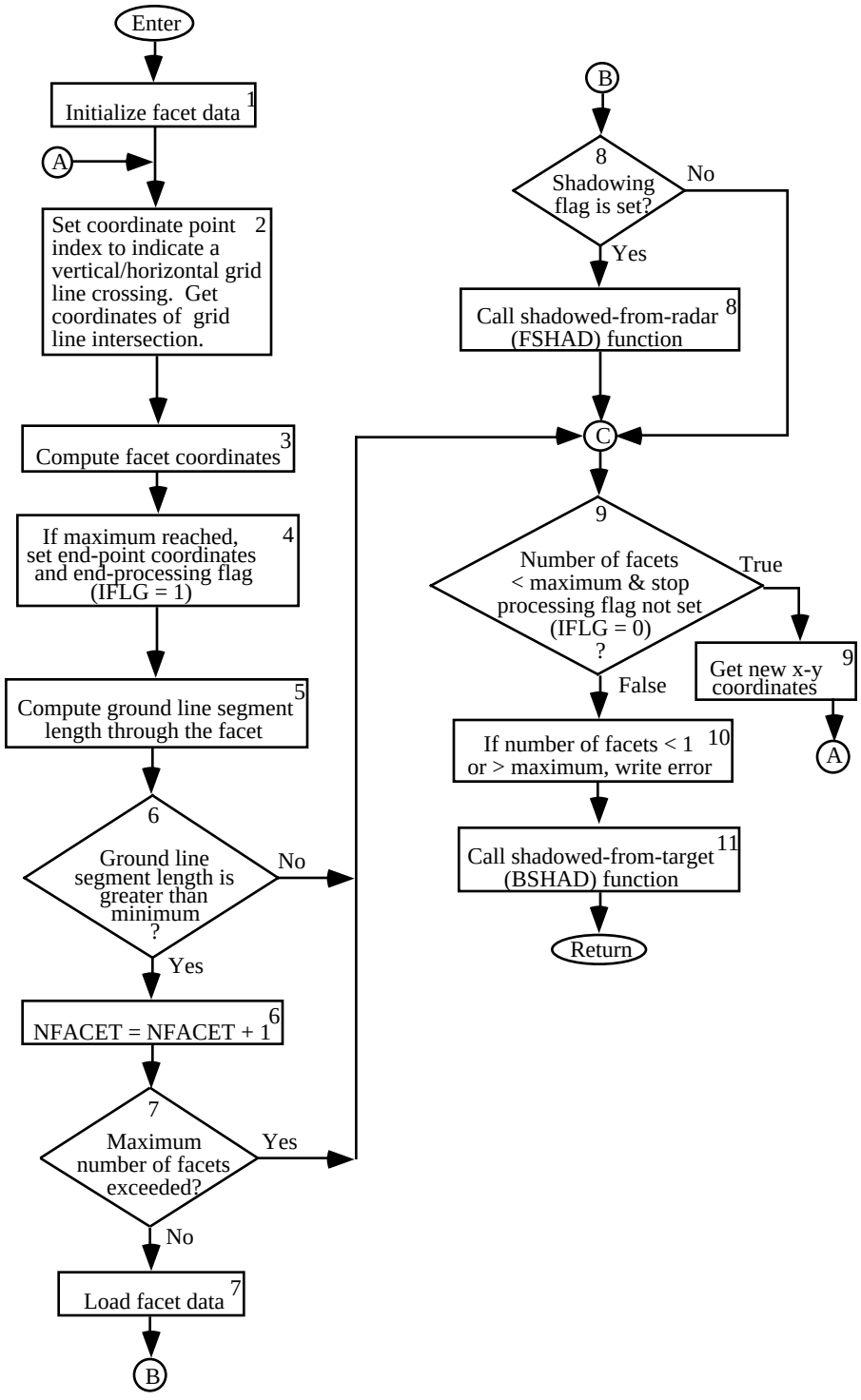

FIGURE 2.13-10. Subroutine FACET Logic Flow Chart.

Block 1. This block represents a call to subroutine FACIN which determines the initial, or near-end ground line point below the site, the corner coordinates of the last participating facet, and the first ground line intersection with a grid line. Details of this process are shown in Figure 2.13-11.

Block 2. An index variable is set to indicate whether the ground line will intersect the facet at either a horizontal or vertical grid line. If the closest intersection point in the x-direction is with a vertical grid line, then the index will be set to 1. The coordinates of the far-end of the ground line segment are set to the grid line intersection coordinates as indicated in Equation [2.13-8].

Block 3. The upper right-hand corner coordinates of the current facet are computed by rounding the coordinates of the midpoint of the ground line segment to the highest integer as shown in Equation [2.13-9].

Block 4. If the corner coordinates computed in block 4 are greater than or equal to the corner coordinates of the last participating facet computed in block 1, then these are set to the endpoint coordinates (as shown in Equation [2.13-10]), and a stop-processing flag (IFLG) is set.

Block 5. The ground line segment length through the current facet is computed as in Equation [2.13-11].

Block 6. If the ground line segment length through the facet is greater than a minimum of 0.01 (in grid units) then the facet is counted as a participating facet element.

Block 7. If the current number of facets has not exceeded the array-size maximum number of 80, then facet data is loaded into a set of data arrays for use in the multipath computations. This data includes the ground line segment length through the facet, the RMS surface roughness, and a terrain type indicator flag. The transverse and longitudinal tilts and facet heights are also computed here. These operations are not described because this code is currently used only with flat terrain.

Block 8. If the shadowing flag has been set by the user, a call is made at this point to the forward shadowing subroutine FSHAD which determines whether the facet surface is visible from the radar site. This routine is not described because it will always yield no shadowing for flat terrain.

Block 9. If the current facet count has not exceeded the maximum number of 80 and the stop-processing flag (from block 4) has not been set, then the far-end ground line segment point coordinates are transferred to the near-end coordinates and the far-end coordinates are computed by adding the x and y direction increments to the new near-end coordinates. This process is described in Equation [2.13-13].

Block 10. If the final facet count is greater than the maximum number of 80, then the number of participating facets is set to 80 and a warning message is written and a flag is set indicating the condition. If no participating facets were found, then a warning message is written and a flag is set indicating the condition.

Block 11. If the shadowing flag has been set by the user, a call is made at this point to the backward shadowing subroutine BSHAD which determines which facet surfaces are visible from the target. This routine is not described because the current use of only flat terrain.

Figure 2.13-11 shows the logic flow chart for subroutine FACIN. The numbered blocks in the flow chart are discussed below.

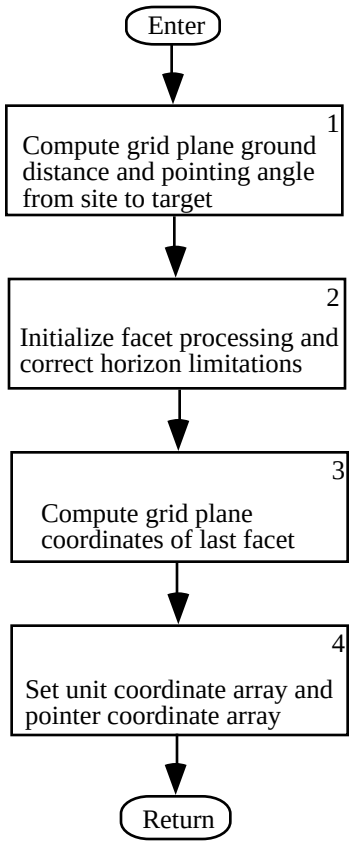

FIGURE 2.13-11. Subroutine FACIN Logic Flow Chart.

Block 1. The grid plane coordinate differences between the site and the target are computed and used to compute ground range from the radar site to the target as shown in Equation [2.13-1]. The site-to-target ground range and the grid plane pointing angles are computed.

Block 2. The coordinates of the first point (located directly under the radar site) are set. A check is also made to determine if the ground range to the target is horizon limited. If not, the coordinates of the end of the ground line are set to the target location. If the range is horizon limited, then the coordinates of the endpoint are computed. See Equations [2.13-2] and [2.13-3].

Block 3. The grid plane corner coordinates of the facet containing the end of the ground line are computed as shown in Equation [2.13-4]. The algebraic sign of the grid plane coordinate differences are computed at this point for future computational convenience.

Block 4. Set up the unit coordinate array YNC(I,J) to give vertical and horizontal distances from one grid line intercept to the next as described in Equation [2.13-7]. Also set up the pointer coordinate array POINT(I,J) to give the coordinates of the nearest *x* and *y* facet intersections as described in Equations [2.13-5] and [2.13-6].

Figure 2.13-12 shows the logic flow chart for subroutine MLTRSP. The numbered blocks in the flow chart are discussed below.

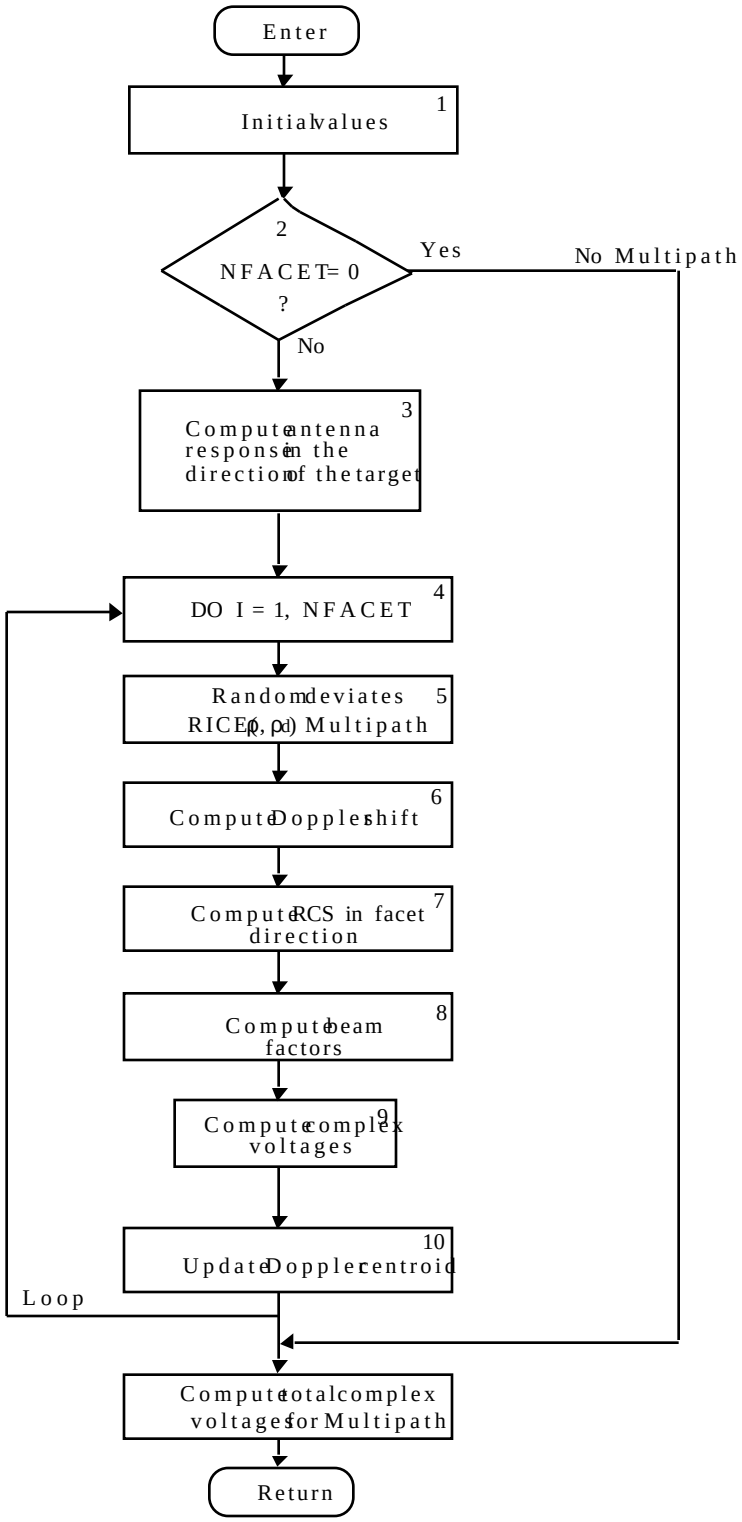

FIGURE 2.13-12. Subroutine MLTRSP Logic Flow Chart.

Block 1. MLTRSP first initializes real and complex variables associated with signal voltages and the Doppler centroid. The target coordinates relative to the site are also computed for use in antenna response calculations.

Block 2. This block represents a check to determine if there were any participating facets found. If not, the multipath response algorithm is skipped and the voltage and Doppler values initialized to zero in block 1 are returned.

Block 3. In preparation for use as a factor in the radar range equation, the sum and difference channel antenna response in the direction of the target is calculated. This step represents a call to the antenna response function FEND contained in another functional element. The gain value returned at this point is represented by the G_T's in Equations [2.13-43] and [2.13-44].

Block 4. This block marks the beginning of a processing loop over all participating facet elements.

Block 5. A composite multipath response consists of coherent and noncoherent components. Computation of the composite response begins by examining the results of the diffuse reflection coefficient calculations performed in subroutine MULTIP. If the diffuse reflection coefficient for the current facet is zero, then only the specular component is present and is transferred to the multipath factor ZTRI for use in the radar range equation. If a diffuse component is present, then the specular component is used as a bias in a Ricean draw. The result of the Ricean draw is the range equation multipath factor.

Block 6. A Doppler frequency at each facet is computed from Equations [2.13-46] and [2.13-47]. This Doppler frequency depends on the relative geometry of the site, target and facet element.

Block 7. The radar cross section (RCS) of the target relative to the facet is determined using the special function AZEL to compute the target aspect and the two-dimensional table lookup function TLU2.

Block 8. The sum and difference channel antenna responses in the direction of the current facet is computed next with a call to FEND. These gains are represented by the $G_{F_i}{}'s$ in Equations [2.13-43] and [2.13-44].

Block 9. This step represents an accumulation of the sum and difference channel gains at each facet element. These quantities are shown as the summations inside the square brackets of Equation [2.13-45].

Block 10. This block accumulates the weighted Doppler frequencies at each facet. This operation is given by Equation [2.13-48].

Block 11. After all facets have been processed, the sum and difference channel voltages for the multipath response are computed by completing the radar range equation given by [2.13-45].

Native Multipath Input and Output Data

The outputs of this functional element are the sum and difference channel voltages of the multipath signal and Doppler centroid of the multipath return as given in Table 2.13-3. User Inputs which affect native mode multipath are given in Table 2.13-4.

TABLE 2.13-3. Native Mode Multipath Outputs.

Variable Name	Description
SUML1	Sum channel multipath voltage
DF1ML	Azimuth difference channel multipath voltage
DF2ML	Elevation difference channel multipath voltage
DOPPLER	Doppler centroid of the multipath return

TABLE 2.13-4. User Inputs for Native Mode Multipath.

Common Name	Variable Name	Description
PROGC	RTERN	Digital terrain option flag (default = 0)
PROGC	XKCLFL	Clutter and multipath activation flag
PROGC	TTYPE	Terrain type (default = 3, grass)
PROGC	TERRF	Terrain roughness (default = 1.0000 m)
PROGC	TERZ	Terrain height (default = 0)
PROGC	WET	Wet terrain flag
PROGC	SNOW	Snow on terrain flag
PROGC	SITES	User-defined site locations; (X,Y,Z) for 200 sites
MULC	DECI	Dielectric coefficient table
MULC	DECR	Dielectric coefficient table
RDRD	XHPANA	Azimuth half-power angle; non-circular beam
RDRD	XHPANE	Elevation half-power angle; non-circular beam
RDRD	XHPANG	Half-power angle; circular beam
RDRD	XICALC	Antenna calculation flag
RDRD	XICIRC	Flag for beam shape; 0 = circular, 1 = non-circular
RDRD	XPWRTX	Transmitter power, tracker
RDRD	XPWTX	Pulse width of radar transmitter
RDRD	XROTB	Array of rotation angles for four beams
RDRD	XSQUANG	Array of squint angles for four beams
RDRD	XWVLTX	Wavelength of radar transmitter
TGTS	SIGTBL	Radar cross section (signature) table

Tables 2.13-3 through 2.13-9 summarize the input and output variables for each of the subroutines listed in Table 2.13-2 that implement the native multipath design.

TABLE 2.13-5. Subroutine MULTIP Inputs and Outputs.

SUBROUTINE: MULTIP

Inputs			Outputs		
Name	**Type**	**Description**	**Name**	**Type**	**Description**
IRADFL	Common FLAGS	Radar type flag, 1=ACQ, 2=TRACK, 3=SEEK, 4=ILLUM.	FACZMC	Common MPATHC	Factor used in the Fresnel reflection Coefficient
BOREEL	Common FREND	Boresight elevation angle	RHOM	Common MPATHC	Array of 80 specular multipath reflection Coefficients

TABLE 2.13-5. Subroutine MULTIP Inputs and Outputs. (Contd.)

SUBROUTINE: MULTIP

Inputs			Outputs		
Name	**Type**	**Description**	**Name**	**Type**	**Description**
HPANGE	Common FREND	Elevation half-power angle	R2FACT	Common MPATHR	Ground line distance from site to center of facet
WVLTX	Common GRADAR	Wavelength of radar transmitter	IF4	Common SIMVI	Terrain type of a particular facet
C0	Common MPATHR	2*PI*SQRT(2)/100*WL (Constant)	ISHAD	Common SIMVI	Terrain shadowing flag
C01	Common MPATHR	4*SQRT(PI) (Constant)	NN	Common SIMVI	Facet number of first non-zero RHO or RHOD
C3	Common MPATHR	PW*C/2 (Constant) Distance traveled at the speed of light in one-half of a pulse width	ETA	Common SIMVR	Elevation angles of facets
DC	Common MPATHR	Array of 9 ground correlation lengths	RHOD	Common SIMVR	Array of diffuse multipath reflection coefficients
IFACER	Common MSGERR	Error in subroutine FACET flag	THETAI	Common SIMVR"	Elevation angles from facet to site

TABLE 2.13-5. Subroutine MULTIP Inputs and Outputs. (Contd.)

SUBROUTINE: MULTIP

Inputs			Outputs		
Name	**Type**	**Description**	**Name**	**Type**	**Description**
DECI DECR	Common MULC	Dielectric coefficient tables			
WAVEHT	Common MULC	Significant wave height			
SNOW	Common PROGC	Snow on terrain flag			
WET	Common PROGC	Wet terrain flag			
KEYSAM	Common PROGVI	Missile number			
RTSH	Common RELSIT	Horizontal distance from target to site			
ZSJ	Common RUNVR	TTR Antenna Coordinate in ICS			
NFACET	Common SIMFLG	Number of facets between site and target			
IFACET	Common SIMVI	Array of facet information			
POS	Common SIMVR	Array of height, length, and site elevation			
PSIT	Common TARG	Target roll angle			
XT YT ZT	Common TARG	Target location coordinates			
TSCLMT	Common TERNDR	Facet edge scaling length			
RHOM	Common MPATHC	Array of 80 specular multipath reflection coefficients			
XSE YSE ZSE	Common MPATHR	Coordinates of the radar site			
RHOD	Common SIMVR	Array of diffuse multipath reflection coefficients			
ETA	Common SIMVR	Elevation angles of the facets			
PLR	Common RDRD	Polarization of radar signal			

TABLE 2.13-6. Subroutine MULTIN Inputs and Outputs.

SUBROUTINE: MULTIN

Inputs			Outputs		
Name	**Type**	**Description**	**Name**	**Type**	**Description**
BOREAZ BOREEL	Common FREND	Boresight azimuth and elevation angles	RHOM	Common MPATHC	Array of 80 specular multipath reflection coefficients
PWTX	Common GRADAR	Transmitter pulse width	C0	Common MPATHR	2*PI*SQRT(2)/ 100*WL (constant)
WVLTX	Common GRADAR	Transmitter wavelength	C01	Common MPATHR	A*SQRT(PI) (constant)
XSJ YSJ ZSJ	Common RUNVR	Current radar site coordinates in ICS	C3	Common MPATHR	PW*C/2 (constant) Distance traveled at the speed of light in one-half of a pulse width
SMAX	Common RUNVR	Absolute sum pattern boresight response	DC	Common MPATHR	Array of 9 ground correlation lengths
TSCLMT	Common TERNDR	Facet edge scaling length	XSE YSE ZSE	Common MPATHR	Coordinates of radar site
			SMAX	Common RUNVR	Absolute sum pattern boresight response
			RHOD	Common SIMVR	Array of diffuse multipath reflection coefficients

TABLE 2.13-7. Subroutine FACET Inputs and Outputs.

SUBROUTINE: FACET

Inputs			Outputs		
Name	**Type**	**Description**	**Name**	**Type**	**Description**
XSF YSF ZSF	Argument	Radar site coordinates	IFACER	Common MSGERR	Error in subroutine FACET flag
XTF YTF ZTF	Argument	Target location coordinates	IFACET	Common SIMVI	Table of facet information
SINB COSB	Common MCLUT	Sine and cosine of the ground-plane azimuth of the target	INDX	Common SIMVI	Index into POINT array
POINT	Common MCLUT	Array containing coordinates used in locating facet edge - ground line intersections	POS	Common SIMVR	Array of height, length and site elevation

TABLE 2.13-7. Subroutine FACET Inputs and Outputs. (Contd.)

SUBROUTINE: FACET

Inputs			Outputs		
Name	**Type**	**Description**	**Name**	**Type**	**Description**
SYNEX SYNEY	Common MCLUT	Sign of the XY-direction to the target	Z1 Z2	Common SIMVR	Altitude of the facet at the near and far edges
X1 Y1	Common MCLUT	Coordinates of the first facet ground line intersection point			
XTE YTE	Common MCLUT	Coordinates of the target location in TSCALE units			
YNC	Common MCLUT	Array containing pointing directions			
X2 Y2	Common MCLUT	Coordinates of the second facet - ground line intersection point			
LUNLP	Common RUNVI	Line printer unit number			
NFACET	Common SIMFLG	Number of facets between site and target			
INDX	Common SIMVI	Index into POINT array			
ISHAD	Common SIMVI	Terrain shadowing flag			
LPT KPT	Common SIMVI	Integer coordinates of the last participating facet			
IVAL	Common TERNDR	Array of facet definition parameters			
TSCLMT	Common TERNDR	Facet edge scaling lengths			

TABLE 2.13-8. Subroutine FACIN Inputs and Outputs.

SUBROUTINE: FACIN

Inputs			Outputs		
Name	**Type**	**Description**	**Name**	**Type**	**Description**
XSF YSF ZSF	Argument	Radar site coordinates	SINB COSB	Common MCLUT	Sine and cosine of the ground plane azimuth of the target
XTF YTF ZTF	Argument	Target location coordinates	POINT	Common MCLUT	Array containing coordinates used in locating facet edge - ground line intersections

TABLE 2.13-8. Subroutine FACIN Inputs and Outputs.(Contd.)

SUBROUTINE: FACIN

Inputs			Outputs		
Name	**Type**	**Description**	**Name**	**Type**	**Description**
CHORIZ	Common CONST	Horizon constant	SYNEX SYNEY	Common MCLUT	Sign of the XY-direction to target
EPSILN	Common CONST	Small number used in computations	X1 Y1	Common MCLUT	Coordinates of the end of the ground line segment
ZSJ	Common RUNVR	TTR antenna z-coordinate in ICS	XTE YTE ZTE	Common MCLUT	Coordinates of the target location in TSCALE units
TSCLMT	Common TERNDR	Facet edge scaling lengths	YNC	Common MCLUT	Array containing pointing directions
			IFACTI	Common MSGERR	Target out of terrain flag
			NFACET	Common SIMFLG	Number of facets between site and target
			KPT LPT	Common SIMVI	Integer coordinates of last participating facet
			XMAX YMAX	Argument	Coordinates of the maximum range to the target

TABLE 2.13-9. Subroutine MLTRSP Inputs and Outputs.

SUBROUTINE: MLTRSP

Inputs			Outputs		
Name	**Type**	**Description**	**Name**	**Type**	**Description**
RHOM	Common MPATHC	Specular multipath reflection coefficient	SUML1	Argument	Sum channel multipath voltage
RHOD	Common SIMVR	Diffuse multipath reflection coefficient	DF1ML DF2ML	Argument	Azimuth and elevation difference channel multipath voltage
XT YT ZT	Common TARG	Target location coordinates	DOPPLR	Argument	Doppler centroid of the multipath return
SIGTBL	Common TGTS	Radar cross section (signature) table			
NFACETS	Common SIMFLG	Number of facets between site and target			
XSJ YSJ ZSJ	Common RUNVR	Coordinates of radar site			
RTS	Common RELSIT	Distance from target to site			
ATNMTI	Common GRADAR	MTI filter attenuation factor			
PWRTX	Common GRADAR	Average transmitter power			
WVLTX	Common GRADAR	Transmitter wavelength			
BMGAIN	Common FREND	Gain of individual beams			
BOREAZ BOREEL	Common FREND	Boresight azimuth and elevation angles			
HPANG	Common FREND	Half-power angle for a circular beam			
HPANGA HPANGE	Common FREND	Half-power angles for non-circular beam (azimuth, elevation)			
HPOWER	Common FREND	Half-power angle			
ICALC	Common FREND	Antenna calculation flag: 0=calculate, 1=look-up gain, 2=look-up antenna pattern			
ICIRC	Common FREND	Antenna type flag: 0=Circular cross section, 1=non-circular cross-section			

TABLE 2.13-9. Subroutine MLTRSP Inputs and Outputs. (Contd.)

SUBROUTINE: MLTRSP

Inputs			Outputs		
Name	**Type**	**Description**	**Name**	**Type**	**Description**
ROTB	Common FREND	Array of four rotation angles for the monopulse beams			
SNORM	Common FREND	Sum gain normalization factor			
SQANG	Common FREND	Array of squint angles for the four monopulse beams			

GRACE Multipath Software Design

A single subroutine, GRCMLT, is used to implement the GRACE multipath design. The call hierarchy within the RF sensor model, a logical flow chart of the subroutine implementation, and the input and output data variables associated with the subroutine are described below.

GRACE Multipath Subroutine Design

The subroutine call hierarchy diagram for the GRACE multipath implementation is shown in Figure 2.13-13. This diagram shows the calling sequence of the GRACE multipath functional element within the entire ESAMS model structure. Subroutine GRCMLT which implements the functional element appears in the shaded block. Subroutines which use the GRACE multipath data output appear in filled in blocks.

Subroutine GRCMLT is called from subroutine CLUTTR to provide the GRACE option for multipath contributions to the signal voltages for the sum channel, the difference channel for azimuth, and the difference channel for elevation, as well as the multipath contribution to the Doppler centroid.

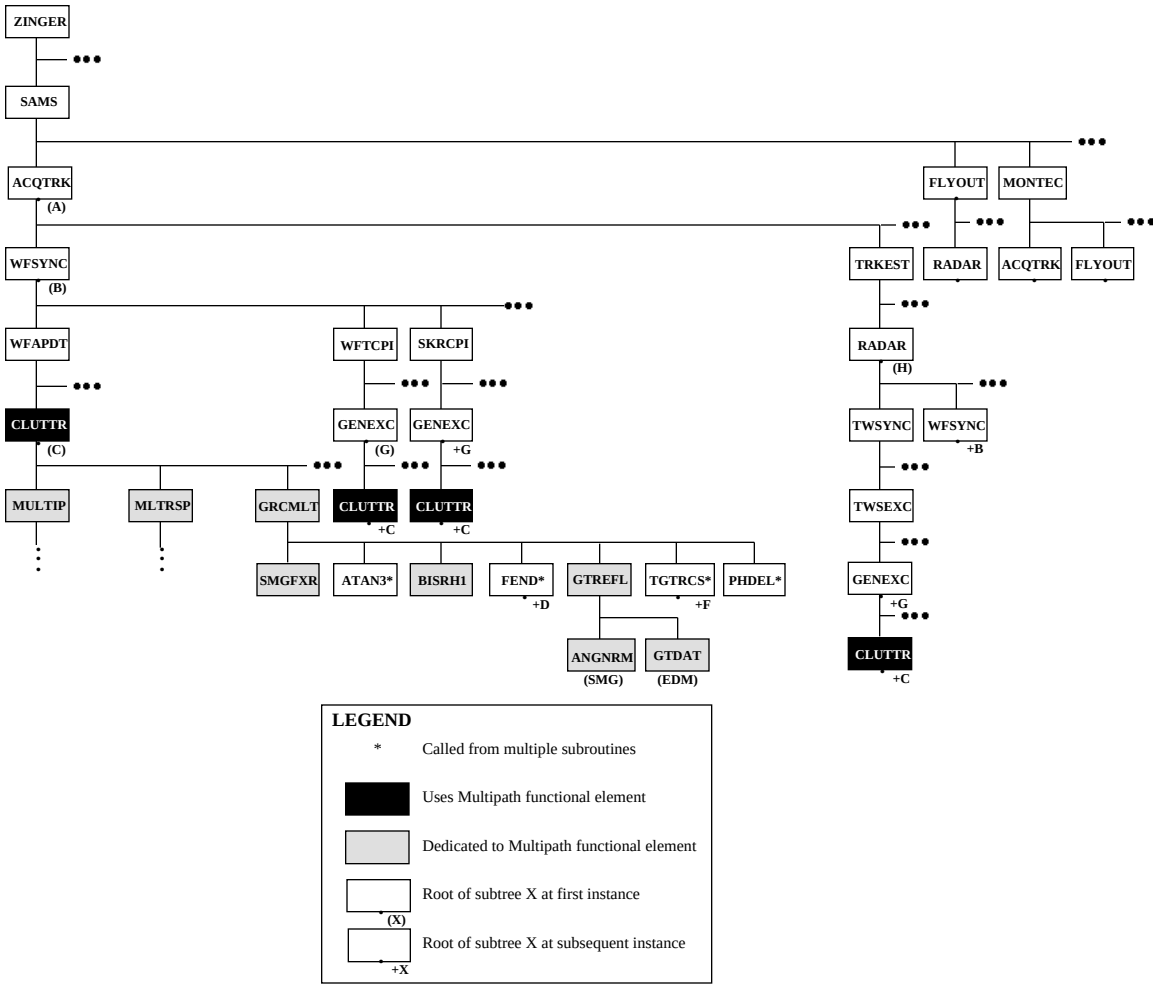

FIGURE 2.13-13. GRACE Multipath Subroutine Call Hierarchy Diagram.

GRACE Multipath Logic Flow

The block diagram in Figure 2.13-14 shows the functions that determine the impact of GRACE multipath effects on target tracking and acquisition. Each block contains a specific function and the subroutine in which that function will occur. The names of the subroutines are in parentheses.

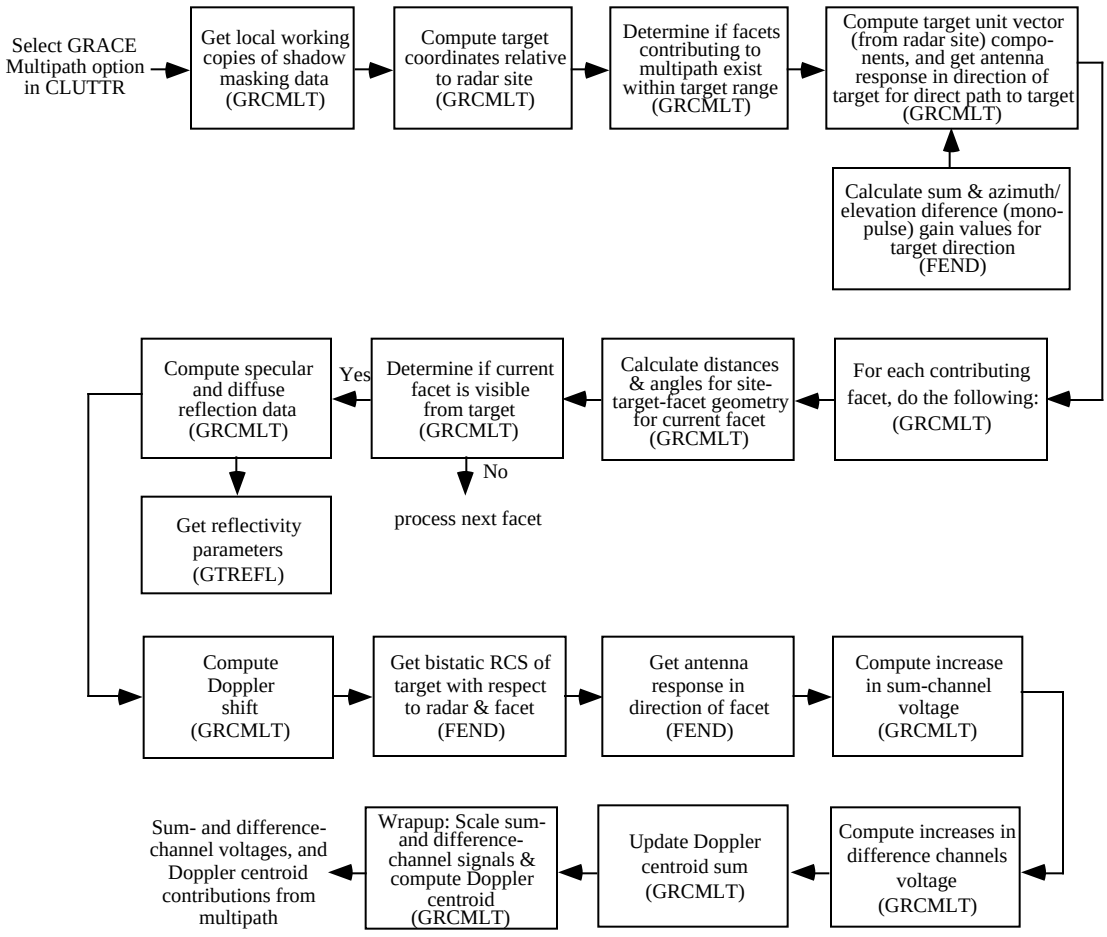

FIGURE 2.13-14. GRACE Multipath Block Diagram.

Figure 2.13-15 shows the logic flow chart for the subroutine. The numbered blocks in the flow chart are discussed below.

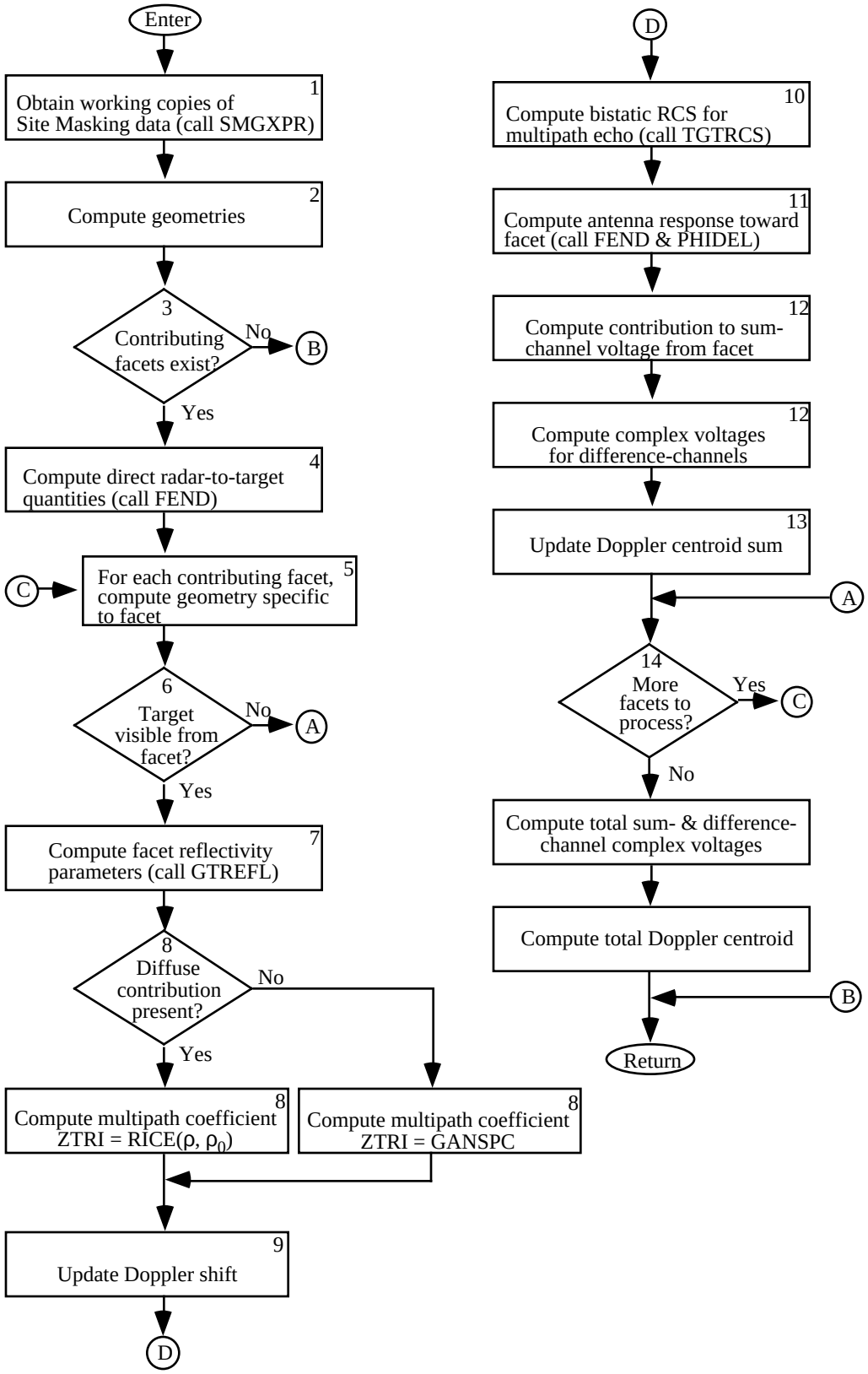

FIGURE 2.13-15. Subroutine GRCMLT Logic Flow Chart.

Block 1. This block represents an initialization step where a call to the special subroutine SMGXFR which transfers working copies of the SMG masking data to local arrays, the azimuthal increment of the site mask radials is computed using Equation [2.13-49] and voltage and Doppler centroid variables are initialized to zero.

Block 2. Geometric quantities are initialized at this step. The target coordinates relative to the site are computed, bearing and elevation angles of the target from the site are calculated and the radial facet number is computed using Equation [2.13-31], and data is retrieved with a call to the subroutine BISRH1. A call to BISRH1 returns NFACET, the number of facets along the multipath radial.

Block 3. This block represents a check to determine if there are any facets. If not, the rest of the multipath algorithm is skipped and the voltage and Doppler values initialized to zero in block 1 are returned.

Block 4. This block represents a call to the antenna response function FEND. This call computes the sum and difference channel antenna response gains in the direction of the target as in Equations [2.13-69] and [2.13-70].

Block 5. This block marks the beginning of a loop for processing all facets contributing to multipath along the radial. Referencing the geometry in Figure 2.13-4, facet processing begins by computing the slant ranges R_1 from the target to the facet midpoint and R2 from the radar site to the facet midpoint and the grazing angles θ_1 between R_1 and d_2, and θ_2 between R_2 and d_2.

Block 6. If the grazing angle θ_1 is greater than zero, then the facet surface is visible from the target. If it is less than zero the facet is shadowed from the target and the facet will not be considered for further multipath processing.

Block 7. The effective radial length of the facet is computed from Equation [2.13-57], the effective scattering area is calculated using equation [2.13-58] and the reflectivity of the facet is obtained from a call to GTREFL. GTREFL returns the diffuse and specular reflection coefficients and the phase shift of the ground reflection as a function of bearing and range from the radar site.

Block 8. The diffuse and specular reflection gain portions of the sum and difference channel voltages in Equation [2.13-63] are computed. If the diffuse reflection gain is zero, then only a specular component exists and is transferred to the multipath coefficient ZTRI for use in the radar range equation. If the coefficient is nonzero then a Ricean draw is performed on the specular bias.

Block 9. The Doppler shift of the target return in the direction of the current facet is computed next by first computing the vector directed from the radar to the facet, and then the vector directed from the facet to the target. The Doppler shift is computed as shown in the large brackets in the numerator of Equation [2.13-71].

Block 10. The bistatic radar cross section (RCS) of the target is obtained next from a call to subroutine TGTRCS. This call generates the RCS of the target relative to the facet.

Block 11. The sum and difference channel antenna responses in the direction of the current facet is computed next with a call to FEND. These gains are represented by Equations [2.13-69] and [2.13-70].

Block 12. This step represents an accumulation of the sum and difference channel voltages at each facet element. These quantities are shown in Equation [2.13-63].

Block 13. This block accumulates the weighted Doppler frequencies at each facet. This operation is given by Equation [2.13-71].

Block 14. After all facets have been processed, the sum and difference channel voltages for the multipath response are computed by completing the radar range equation given by [2.13-45].

GRACE Multipath Input and Output Data

The outputs of this functional element are the sum and difference channel voltages of the multipath signal and the Doppler centroid of the multipath return as given in Table 2.13-10. User inputs which affect GRACE mode multipath are given in Table 2.13-11.

TABLE 2.13-10. GRACE Mode Multipath Outputs.

Variable Name	Description
SUML1	Sum channel multipath voltage
DF1ML	Azimuth difference channel multipath voltage
DF2ML	Elevation difference channel multipath voltage
DOPPLER	Doppler centroid of the multipath return

TABLE 2.13-11. User Inputs for GRACE Mode Multipath.

Common Name	Variable Name	Description
PROGC	SITES	User-defined site locations; (X,Y,Z) for 200 sites
RDRD	XHPANA	Azimuth half-power angle; non-circular beam
RDRD	XHPANE	Elevation half-power angle; non-circular beam
RDRD	XHPANG	Half-power angle; circular beam
RDRD	XICALC	Antenna calculation flag
RDRD	XICIRC	Flag for beam shape; 0 = circular, 1 = non-circular
RDRD	XPWRTX	Transmitter power, tracker
RDRD	XROTB	Array of rotation angles for four beams
RDRD	XSQUANG	Array of squint angles for four beams
RDRD	XWVLTX	Wavelength of radar transmitter
TGTS	SIGTBL	Radar cross section (signature) table

Other user inputs are required for the Site Mask Generator, but those are beyond the scope of this section.

Table 2.13-12 summarizes the input and output variables for subroutine GRCMLT that implements the GRACE multipath design.

TABLE 2.13-12. Subroutine GRCMLT Inputs and Outputs.

SUBROUTINE: GRCMLT					
Inputs			**Outputs**		
Name	**Type**	**Description**	**Name**	**Type**	**Description**
XT YT ZT	Common TARG	Target location coordinates	SUML1	Argument	Sum channel multipath voltage
SIGTBL	Common TGTS	Radar cross section (signature) table	DF1ML DF2ML	Argument	Azimuth and elevation difference channel multipath voltage
XSJ YSJ ZSJ	Common RUNVR	Coordinates of radar site	DOPPLR	Argument	Doppler centroid of the multipath return
RTS	Common RELSIT	Distance from target to site			
ATNMTI	Common GRADAR	MTI filter attenuation factor			
PWRTX	Common GRADAR	Average transmitter power			
WVLTX	Common GRADAR	Transmitter wavelength			
BMGAIN	Common FREND	Gain of individual beams			
BOREAZ BOREEL	Common FREND	Boresight azimuth and elevation angles			
HPANG	Common FREND	Half-power angle for a circular beam			
HPANGA HPANGE	Common FREND	Half-power angles for non-circular beam (azimuth, elevation)			
HPOWER	Common FREND	Half-power angle			
ICALC	Common FREND	Antenna calculation flag: 0=calculate, 1=look-up gain, 2=look-up antenna pattern			
ICIRC	Common FREND	Antenna type flag: 0=Circular cross section, 1=non-circular cross-section			
ROTB	Common FREND	Array of four rotation angles for the monopulse beams			
SNORM	Common FREND	Sum gain normalization factor			
SQANG	Common FREND	Array of squint angles for the four monopulse beams			
IRADFL	Common FLAGS	Radar-type flag			

2.13.4 Assumptions and Limitations

Native Multipath Assumptions and Limitations

The native mode implementation of multipath is not currently mated to digitized terrain; thus, it is limited to the default flat-earth terrain, even though the code is designed for digitized terrain.

No diffraction is modeled.

Specular multipath includes only returns from direct-indirect (one bounce) round-trip paths; the indirect-indirect path (two bounces) is not included.

Multipath is not used for missile seeker radars.

All calculations use single precision arithmetic.

Small angle approximations are used for the depression angles from the radar and target to the terrain bounce points and for the associated grazing angles. These approximations replace the angle's sine and tangent with the angle itself (in radians), and the cosine with 1. These approximations have relative errors of less than 0.5% for angles up to 1/10 of a radian (5.73 degrees).

GRACE Multipath Assumptions and Limitations

The GRACE multipath implementation uses site mask data, a much-condensed representation of the terrain data. These data are arranged in radials from the radar site, nominally 0.5 degrees apart. Multipath returns are contributed only from the radial nearest to the bearing of the target.

The GRACE multipath implementation uses the Environmental Characteristics Package for values of the magnitude and phase shift of the ground reflectivity. Current default values are 0.5 for magnitude and 180 degrees for phase shift; but phase-shift data is not used.

This mode does not require multipath returns to fall within the range gate; thus, multipath effects may be overestimated.

In each illumination patch along the radar, only the second half of the patch is allowed to contribute multipath returns; i.e., only the segment from the midpoint of the patch to the end of the patch farthest from the radar site.

The only multipath effects modeled are the impacts on angle track and Doppler.